Methodology for Identifying Inverter-based Renewable Generation Penetration Threshold in a Power System

by

Hashem A M H S Albhrani

A Thesis Presented in Partial Fulfillment
of the Requirements for the Degree
Master of Science

Approved April 2020 by the
Graduate Supervisory Committee:

Anamitra Pal, Chair
Keith E. Holbert
Raja Ayyanar

ARIZONA STATE UNIVERSITY

May 2020

ABSTRACT

Energy is one of the wheels on which the modern world runs. Therefore, standards and limits have been devised to maintain the stability and reliability of the power grid. This research shows a simple methodology for increasing the amount of Inverter-based Renewable Generation (IRG), which is also known as Inverter-based Resources (IBR), for that considers the voltage and frequency limits specified by the Western Electricity Coordinating Council (WECC) Transmission Planning (TPL) criteria, and the tie line power flow limits between the area-under-study and its neighbors under contingency conditions. A WECC power flow and dynamic file is analyzed and modified in this research to demonstrate the performance of the methodology. GE's Positive Sequence Load Flow (PSLF) software is used to conduct this research and Python was used to analyze the output data.

The thesis explains in detail how the system with 11% of IRG operated before conducting any adjustments (addition of IRG) and what procedures were modified to make the system run correctly. The adjustments made to the dynamic models are also explained in depth to give a clearer picture of how each adjustment affects the system performance. A list of proposed IRG units along with their locations were provided by SRP, a power utility in Arizona, which were to be integrated into the power flow and dynamic files. In the process of finding the maximum IRG penetration threshold, three sensitivities were also considered, namely, momentary cessation due to low voltages, transmission vs. distribution connected solar generation, and stalling of induction motors. Finally, the thesis discusses how the system reacts to the aforementioned modifications, and how IRG

penetration threshold gets adjusted with regards to the different sensitivities applied to the system.

ACKNOWLEDGMENTS

I am honored and privileged to be a member of Prof. Anamitra Pal's research group as it has enabled me to make a difference to the field of power system engineering. Prof. Pal was my mentor and advisor since my first semester here at Arizona State University. Prof. Pal's advice on both academic and professional life have been extremely valuable for me during my graduate life. His constant support and encouragement, mixed with fairness, considerably enhanced my learning experience. I am grateful to all members of the Pal Lab who were fascinating in helping me in my journey in learning and discovering the various fields and tools in power engineering – a shout-out, in particular, to Reetam Sen Biswas for his help with many of my codes.

I would like to thank Prof. Keith Holbert and Prof. Raja Ayyanar for their interest and willingness to be a member of my thesis committee and for sharing their experience and knowledge in power engineering. Special thanks also to SRP engineers, Philip Augustin and Matthew Rhodes, for their trust and constructive feedback that helped me successfully complete the project.

I am blessed and thankful to have someone like my mother who supported and encouraged me to face every challenge with everything I got and for setting an example for me in the academic field. Having my father in my life inspired me to master what I am doing and give back to my community. Siblings and friends, you were a great support for me when I needed someone to lean on and solve problems. I am grateful for all the people who added something to me and my journey.

TABLE OF CONTENTS

Page

CHAPTER Page

APPENDIX Page

LIST OF TABLES

LIST OF FIGURES

Figure Page

CHAPTER 1
INTRODUCTION

Electricity is the wheel on which the modern world runs, and without it many essential operations and procedures would definitely derail [1]. Since Benjamin Franklin discovered electricity, the world didn't stop utilizing this energy and came up with as many ways of generating it as possible starting from the flying kite he had used to synchronous generators that run on fossil fuels. The demand for electricity increases as technology applications expand and population grows, which leads to overloading the power system and causing unforeseen issues. However, societies have always been concerned with the natural resources that generate this power and the control over their prices and supply. Moreover, the environmental damage caused by emissions produced by conventional generation methods forced many governments to take action to save the environment [2]. This resulted in restrictions on the amount of emissions that were allowed over specific periods of time [3]. The power industry has been affected by this movement towards "clean energy" in the 2000s when utilities were asked to hit specific percentages of renewable energy generations in their areas; for example, California achieved 33% of renewable energy penetration by 2018, 2 years ahead of its schedule [4]. However, renewable energy trend comes with a toll that utilities must pay for before getting them into their systems. The uncertainty that comes with renewable energy generation due to the different unexpected environmental scenarios could cause huge loss of power generation and instability in the system, so new techniques and technology have to be utilized to mitigate them [5], [6], [7]. These issues could conflict with the standards and criteria that are set by the enforcing authorities. Therefore, although renewable energy is a key that can enable many countries to get energy without relying

exclusively on conventional energy sources, many other parameters must be accounted for before turning this key.

1.1 Reliability of the Power Grid

Since the beginning of the 20th century, the expansion of electricity distribution in the U.S. has increased dramatically due to the adaptation of the population to the inventions that require electricity. However, the first large-scale blackout in 1965 pushed the electric utility industry to form an association that maintains and enforces standards and criteria for bulk power system operators in order to maintain its reliability and avoid huge economical and physical damages [8]. The association was called National Electric Reliability Council. Afterwards, another successor entity was formed in 2006 called North American Electric Reliability Corporation (NERC), which monitored North America power grid reliability and proposed suggestions for standards and criteria to be considered for the Western Electricity Coordinating Council (WECC). NERC is a non-profit organization that plays a key role in devising policies that keep the grid in-line with the new technologies that are being added to it, altering the traditional load and generation patterns. NERC does so by updating and adding new guidelines, which enhances situational awareness of power system operators so that they, in turn, can provide the customers more efficient and reliable services. Such entities are very important for a big industry like energy where regulations and standards might conflict with the capability of utilities and customers' needs. Security of the power grid is also considered in NERC analysis programs to reduce the vulnerability of the system against cyber-attacks and/or any potential risks the power grid can face [9].

Having said this, the reliability and security of the power grid is paramount for any power utility and any modification to the existing system, even if it is suggested by NERC

(or WECC for utilities in the West Coast of U.S.), must be tested and verified before it can be implemented in real life [10], [11]. Accordingly, these researches serve the important purpose of checking the performance of a power system with increase in Inverter-based Renewable Generation (IRG) penetration based on specifications requested by power utilities.

1.2 Scope and Objectives

The main objective of this research is to examine the effectiveness of a methodology to find out the maximum IRG penetration threshold while considering the standards and criteria provided by both utilities and power grid entities responsible for reliability and compliance. With the recent push to the continuous increase of renewable generation the power grid in the U.S. as shown in Fig 1.1 below, a question arises regarding the capability for the grid to handle the challenges that come with this trend. Utilities are the deciding party for planning where and by how much they can either modify or add renewable generation. Moreover, system operators try their best to run the system as close to nominal operating conditions as possible. However, outages in power generation happen every now and then, and this scenario puts huge pressure on the grid, causing the cascading failure throughout the system, if the system is not resilient enough [12].

With the increased IRG penetration into the grid, there are two challenges utilities companies face. First, the loss of synthetic inertia if synchronous generators were replaced with IRG units, which could jeopardize the frequency stability of the system [13]. Secondly, the uncertainties and concerns that come with the IRG increase in terms of unexpected weather conditions and the need to make up the losses by alternative ways, which are still being researched in the field of battery storage and governor response [14],

[15]. The power grid community has already done extensive research in simulating high renewable generation cases using various simulation programs. However, the effects that increase of IRG can have on tie-line power flow limits between neighboring areas and the area-under-study has not received significant attention. Lastly, three different sensitivities, namely, momentary cessation due to low voltages, transmission vs. distribution connected solar generation, and stalling of induction motors, were analyzed to determine the ability of the IRG penetration threshold to handle different system conditions.

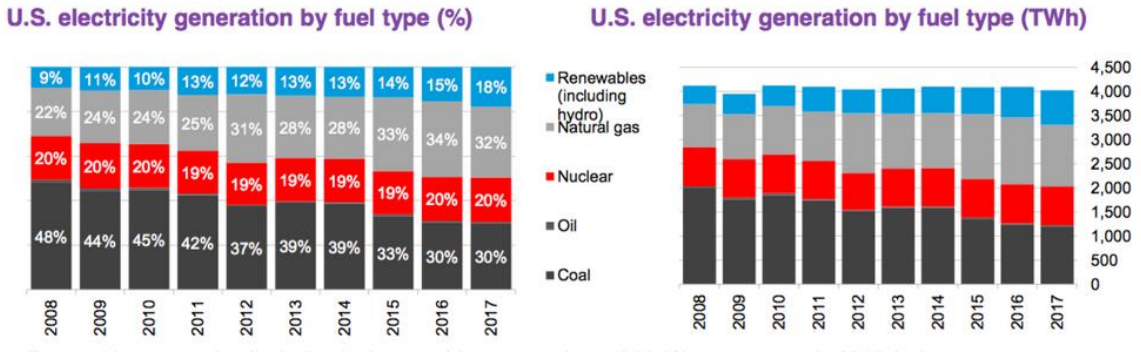

Figure 1.1: Energy sources distribution in the US through the years 2008-2018 in percentages and terawatt-hour (TWh) [16]

The methodology developed in this research depends on existing criteria based on which the case study is tested, and the results reflect how that case performs on the provided contingency cases. Although this methodology is not the only approach to compute the maximum IRG penetration threshold, it shows a realistic and practical way for finding it.

Proposed Methodology Steps:

Phase 1 (Chapter 3):

1. Obtain raw files and list of constraints
2. Create the necessary scripts to check the performance of the original case based on the constraints
3. Add the new proposed IRG units into the system and modify the raw files accordingly
4. Check the performance of the high IRG case. Return to Step (3) if all constraints are passed

Phase 2 (Chapter 4):

1. Apply the three different sensitivities on the original and high IRG case
2. Adjust the IRG penetration threshold in case the constraints are not satisfied

CHAPTER 2

LITERATURE REVIEW

Power grid stability has always been challenging to maintain, and there is no single way to ensure it. The change in load and operating conditions have a significant effect on the system as a whole, especially if the system is interconnected [17]. With small-scale power grid, renewable generation causes fluctuations in the system in terms of frequency, loads, and voltage levels which can be predicted prior to the implementation and can be simulated in a short period of time [18], [19]. However, with a large-scale power grid, the pressure and effect resulted from the renewable generation will make things more complicated and harder to be predicted precisely. Moreover, the introduction of high renewable generation penetration into the system arises new issues of stability such as islanding, power swings, and frequency instability that require in depth studies [20], [21], [22], [23]. Renewable energy leading states are now setting high expectations for the utilities to meet. In California, their plan for 2030 is to reach half of the energy in the state generated by renewable energy [24]. Since California is part of WECC, there has to be studies to follow before achieving the 50% mark by 2030. These studies should keep in mind the criteria and standards set by enforcing entities like WECC and their neighboring utilities. Research labs have developed plans and procedures for utilities to follow in order to obtain both efficient economical and reliable system with the extra renewable generation into the system. In 2017, National Renewable Energy Laboratory (NREL) have come with a guidebook that shows a transmission planning process called Renewable Energy Zone (REZ) [25]. REZ focuses on providing the policy makers a tool to asses and plan their infrastructure investment and maximize its economic aspects while achieving its main

purpose of reduction of air-pollution. This plan is mainly directed to the people who are implementing the proposed increased renewable generation plans, but before accomplishing this step, studies have to be done to show the reliability and resiliency of the system [26]. There are many criteria that determine the reliability of the system. For instance, one way is to look at the historical data for a renewable generation model and see how it reacts to changes in environmental conditions [27]. Alternately, assessment of the reliability of the system can also be done considering transmission expansion planning (TEP). TEP evaluates and decides for the cost and the new techniques applied into the system to handle the reduced system inertia and the increased uncertainties that come with the higher renewable generation penetration into the system [28].

The power industry has also found many ways to simulate the power grid and see how it performs. Some of them involve programming-based tool that considers the regulatory uncertainties and the adaptive transmission planning criteria [29]. Linear programming was another approach to find the suitable economical transmission plans [30]. The linear programming approach includes a linear flow estimation and a new circuit selection for bulk power transmission network. The method showed its ability to guide the planning phase of network where the least and extreme cases where studied, but the method checked few characteristics in consideration without applying contingencies and outages into the system.

Recently, many simulations programs were intensively used in the stability studies domain such as Siemens Power System Simulator for Engineer (PSSE), Dynamic Security Assessment (DSA) Tools “DSATools” and General Electric (GE) Positive Sequence Load Flow (PSLF). These simulations programs provide the user with a unique mathematical

model for any desired dynamical simulation [31], [32]. Siemens PSSE is a common tool used to analyze the response of the systems after a disturbance has been applied [33]. Also, PSSE is common simulator for the eastern states of the U.S., so using it for case studies in those areas would help the researchers to compare different studies using one approach for efficient comparison in the same format. PSSE has also been used outside U.S.; for example, by researchers' studying the photovoltaic integration impacts in the Tunisian grid [34]. Their power grid case was significantly small compared to the power grid interconnections in the U.S., but the results were accurate enough for them to analyze and evaluate the performance and the stability of their grid in a dynamic setting.

DSA Tools is another popular tool used by researchers in the power stability domain. It was one of the early simulation programs to help in analyzing the transient stability and small signal stability of the power grid. In [35], authors used DSATools to come up with an approach to utilize it's real time data collection through DSA Manager, then this data is fed into the system and 3,000 contingency cases are run to find out the performance in terms of stability limits in order to provide preventive actions and/or control procedures. In [36], used DSA Tools was used to analyze the performance of Prony Algorithm in identifying the low frequency oscillations. The simulator showed the validity and the performance of the proposed approach efficiently.

In the western states of the U.S., PSLF is more commonly used [37]. The contingency analysis done in [38] considered intermittent renewable resources continuously during a dynamic simulation. This was made possible through PSLF's in-built coding language, EPCL. PSLF also provides the users with another program that can be used later after running the simulations to visualize the data generated separately or to compare with other

data. Voltage performance can also be monitored in PSLF in cases of simulating wind and solar generation units, as shown in [39]. Moreover, brake insertions were able to be simulated in PSLF in case with high photovoltaic generation, which shows the flexibility that PSLF offers to its researchers [40]. The various modeling options of PSLF and its ability to modify contingency cases gives it a higher rank compared to the other simulation programs, especially when it to comes to renewable energy simulations. PSLF allows creation of many user-defined models for almost all renewable energy cases in addition to the existing accessories, making it a very efficient tool for analyzing and monitoring dynamic simulations and drawing conclusions [41].

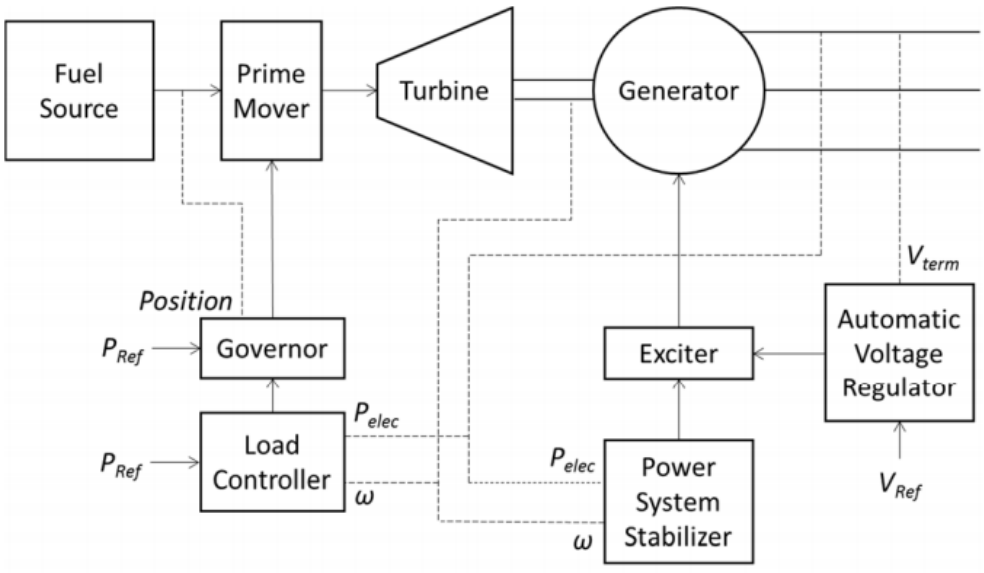

Figure 2.1: An example of a structure of the models for a power plant in PSLF [42]

It is likely that IRG penetration will sky-rocket in the near future (as much as 330 GW for WECC [43]). With these high expectations, utilities in the west coast of U.S. are expected to conduct more research and studies to achieve the goal of WECC without

causing major failures or blackouts. In [44], NREL has provided utilities with plans to follow so that they do not fall behind in the race for high renewable penetration. All in all, there are many ways and tools used to analyze the reliability of the power grid using the standards and concerns given by utilities and enforcing entities. However, renewable generation integration involves doing different types of analysis in order to alleviate the associated concerns as will be described in this research.

CHAPTER 3

IDENTIFICATION OF INVERTER-BASED RENEWABLE GENERATION (IRG) THRESHOLD (PHASE 1)

With the current rapid increasing trend of renewable generation in the U.S., many analytical aspects have to be considered to create a suitable system that can handle the associated challenges and uncertainties. In this chapter, the WECC-24,000 bus system provided by the utility company, SRP will be analyzed to test its ability to satisfy different constraints. Moreover, new locations and capacities of renewable generation units, solar PV, and battery storage, provided by SRP will be used for finding the suitable IRG penetration threshold. Lastly, the standards and criteria requested by WECC and SRP will explained.

Chapter 3 (Phase 1) intends to obtain the maximum IRG penetration threshold for the case study by following the procedure mentioned below:

1. Obtain the power flow file ".sav", dynamic file ".dyd" and contingency list from the utility and adapt it into PSLF environment
2. Create an EPCL script ".p" and switch file ". swt" to run the contingency list provided by the utility
3. Identify the limits and constraints set by the regional entity responsible for power compliance and enforcement, and the tie line limits with the neighboring areas
4. Create an EPCL script ".p" to process the output channel files to check the performance and detect any violations of the standards (post-simulation)
5. Create a Python script ".py" to check if the power flow in the tie lines between areas are exceeding the limits (post-simulation)

6. Run the EPCL script through PSLF with the associated contingency list and the post-simulation scripts to check for any violations
7. Identify the generation units that can be removed from the system and replace them with equivalent IRG units; note that the IRG units may be located at a different bus than the bus from which the conventional unit has been removed
8. Run the EPCL script through PSLF with the associated contingency lists and post-simulation scripts to check for any violations
9. Compare the high IRG case performance with the original case performance. Return to Step 7 if the system exceeds the tie line limits and/or WECC TPL constraints compared to the original case

3.1 Step 1: Obtain the power flow file ".sav", dynamic file ".dyd" and contingency list from the utility and adapt it into PSLF environment.

A power flow ".sav" and a dynamic file ".dyd" case for the WECC was provided by SRP to apply the proposed methodology and find the maximum IRG penetration threshold that it can handle. The system had approximately 24,000 buses. SRP requested to apply the methodology on an area that has 2,750 bus in it with 300 generation units. The area-under-study had a total of 24,750 MW of generation. The power flow file sent by SRP was in a different format; so, this file was directly converted to a ".sav" file and imported into PSLF. After that the dynamic file ".dyd" was run to check if it ran smoothly and matched all the models that existed in the power flow case ".sav".

When the case was initialized for the first time, the process failed, generating an error which stated that there is a mismatch between the dynamic file ".dyd" and the power flow ".sav". The error stated that there was no model for 3 DC (EPCDC) systems. Therefore, identical EPCDC models were written and added for the 3 DC systems. When the case was initialized once more, this error disappeared, but another one surfaced. This one was with regards to the step width of the simulation which was too large for the system to converge. Accordingly, the step width was reduced from 0.004167 seconds to 0.001 seconds to ensure the system converged. After that, another error cropped up, which indicated that the number of space channels were not enough to record all the data. This error was addressed by disabling the record level for load models since it was not necessary for this research. The resulting system after making the aforementioned changes was found to successfully initialize.

The contingency list provided by SRP was in the form of a switch file that ran a simulation for 20 seconds with different type of faults in it. The switch files had two types of contingencies, 8 of the contingencies involve tripping generators (Fig. 3.1), and 48 contingencies involving line faults (Fig. 3.2).

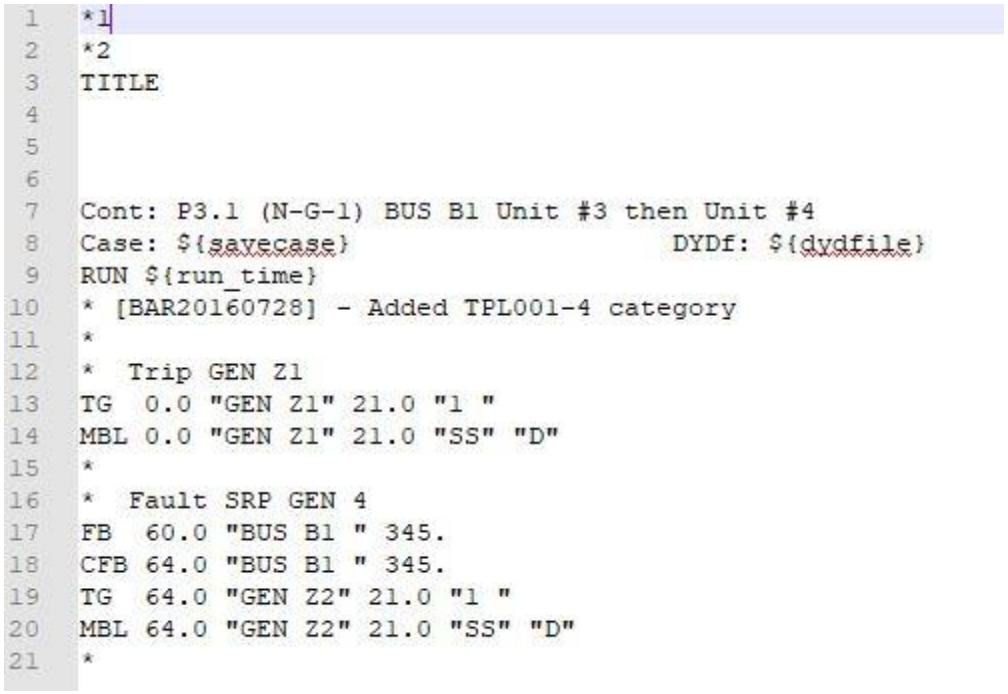

```
*1
*2
TITLE



Cont: P3.1 (N-G-1) BUS B1 Unit #3 then Unit #4
Case: ${savecase}                    DYDf: ${dydfile}
RUN ${run_time}
* [BAR20160728] - Added TPL001-4 category
*
*  Trip GEN Z1
TG  0.0 "GEN Z1" 21.0 "1 "
MBL 0.0 "GEN Z1" 21.0 "SS" "D"
*
*  Fault SRP GEN 4
FB  60.0 "BUS B1 " 345.
CFB 64.0 "BUS B1 " 345.
TG  64.0 "GEN Z2" 21.0 "1 "
MBL 64.0 "GEN Z2" 21.0 "SS" "D"
*
```

Figure 3.1: Switch file provided by SRP for a contingency involve generator

This switch file translates as follows:

- The duration of simulation is 20 seconds
- Interpreted the switch file commands as follows:
    - TG: Trip Generator
    - MBL: Modify Bus Load
    - FB: Faulted Bus
    - CFB: Clear Faulted Bus

```
*1
*2
TITLE



Cont: P7.1 (N-2) Common Tower - Lines GEN1-GEN3 230.0 & GEN1-GEN2 230.0
Case: ${savecase}                    DYDf: ${dydfile}
RUN ${run_time}
* [BAR20160719] - Added TPL001-4 category
*
** Fault on the lines (where common towers exist)
*FL   0.0 "GEN1" 230. "GEN3" 230. "1 " 1 .20 .0 .1 4 4
*FL   0.0 "GEN2" 230. "GEN1" 230. "1 " 1 .80 .0 .1 4 4
*
* Or Fault at nearest bus
FB  0.0 "GEN1" 230.
*   Clear fault at GEN1
CFB 4.0 "GEN1" 230.
*
*
*   Trip FAULT ON TOWER LINE GEN1-GEN3 230.0 & GEN1-GEN2 230.0
DL 4.0 "GEN1" 230. "GEN3" 230. "1 "
DL 4.0 "GEN2" 230. "GEN1" 230. "1 "
*
```

Figure 3.2: Switch file ".swt" provided by SRP for a contingency involve line faults

This switch file translates as follows:

- The duration of simulation is 20 seconds
- Interpreted the switch file commands as follows:
  - FL: Faulted Line
  - FB: Faulted Bus
  - CFB: Clear Faulted Bus
  - DL: Open Line

These switch files were called from the EPCL script ".p" to run them in the simulation.

3.2 Step 2: Create an EPCL script ".p" and switch file ". swt" to run the contingency list provided by the utility

In this step, an EPCL script was created to call the power flow case ".sav" that has the information about generation units and bus locations with their initial parameters and the dynamic file ".dyd" that has the models that control how each element performs. The EPCL script will be anonymous due to copyright.

3.3 Step 3: Identify the limits and constraints set by the regional entity responsible of power compliance and enforcement, and the tie line limits with the neighboring areas

There are three criteria that have to be maintained and considered in this case study. The most recent WECC TPL criteria on voltage and frequency, tie line limits with the neighboring areas, and the mapping of three sensitivities (which will be considered later in Chapter 4 (Phase 2)). These limits verify the ability of the case to handle different scenarios. The details of how each criterion is applied on the generated data is shown below.

3.3.1 WECC Transmission Planning (TPL) Criteria

For a reliable and resilient system, WECC asks utilities to check their systems periodically in simulation programs to different criteria. These criteria are also followed before testing any likely scenarios. These criteria focus on voltage and frequency recovery during contingency cases [45], [46].

WECC transmission planning criteria are summarized as follow:

A. 59.6 Hz frequency deviation criteria: The frequency at any bus cannot remain below 59.6 Hz for more than 6 cycles, as shown in Fig. 3.3.

B. WECC voltage recovery criteria: After the fault has been cleared, the voltage at any bus must recover to 80% of its initial voltage within 20 seconds, as shown in Fig. 3.4.

C. WECC 70% voltage dip criteria: The time duration of the voltage dip below 70% of the initial voltage must not be for more than 30 cycles.

D. WECC 80% voltage dip criteria: The time duration of the voltage dip below 80% of the initial voltage must not be for more than 2 seconds. Fig. 3.5 depicts the 70% voltage dip criteria and the 80% voltage dip criteria, respectively.

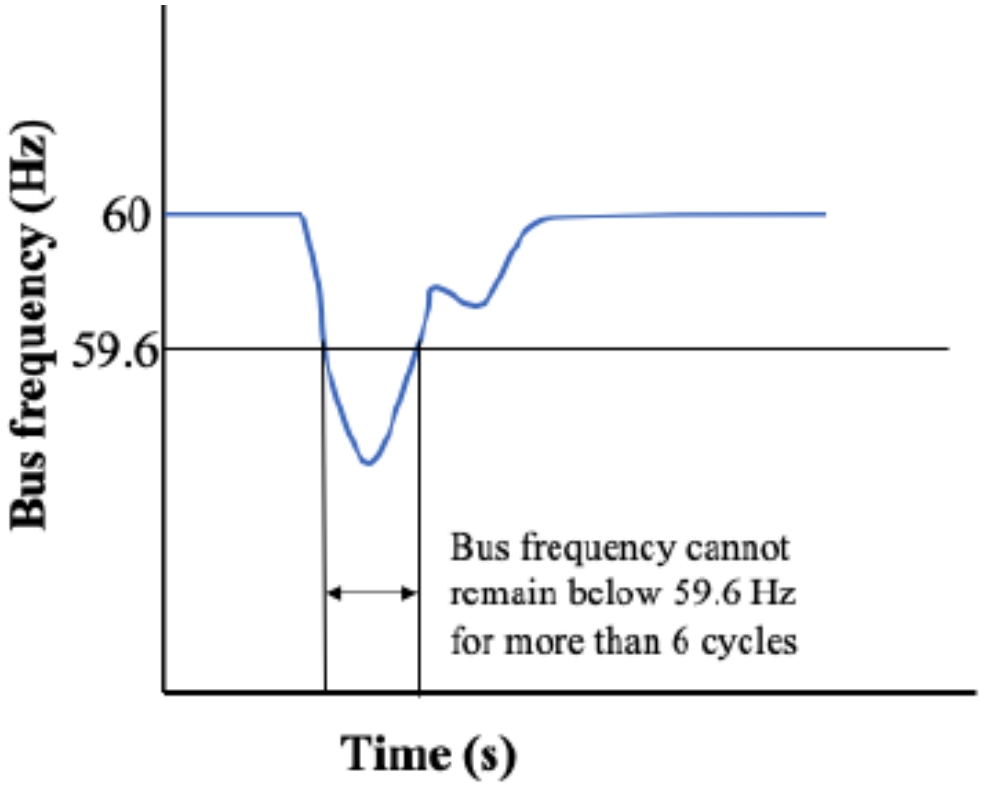

Figure 3.3: WECC 59.6 Hz frequency deviation criteria [45]

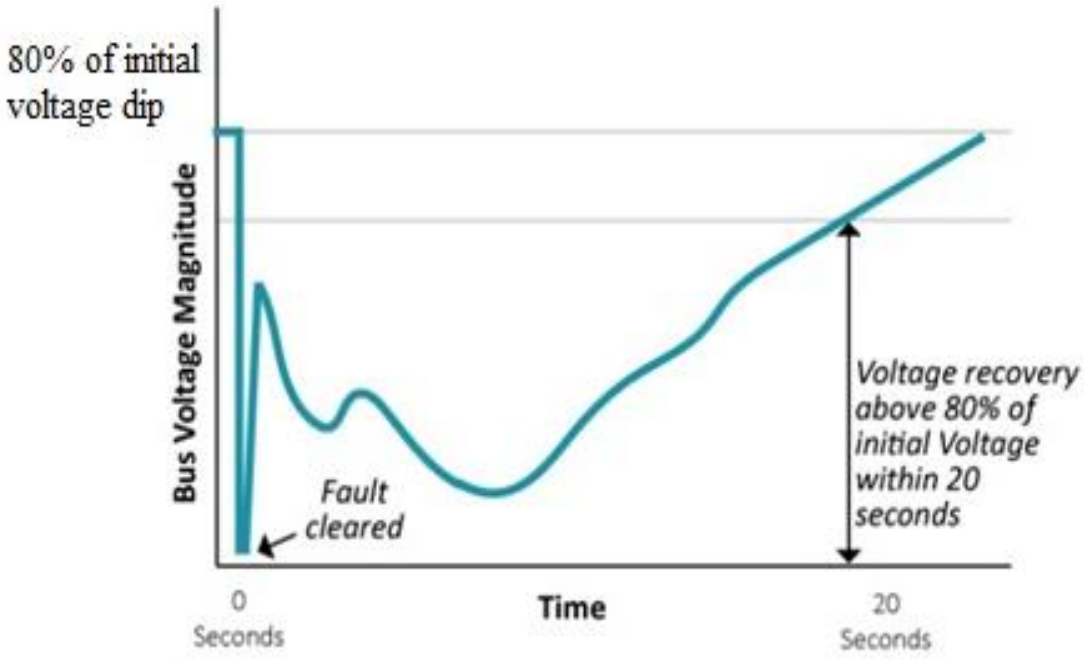

Figure 3.4: WECC voltage recovery criteria [46]

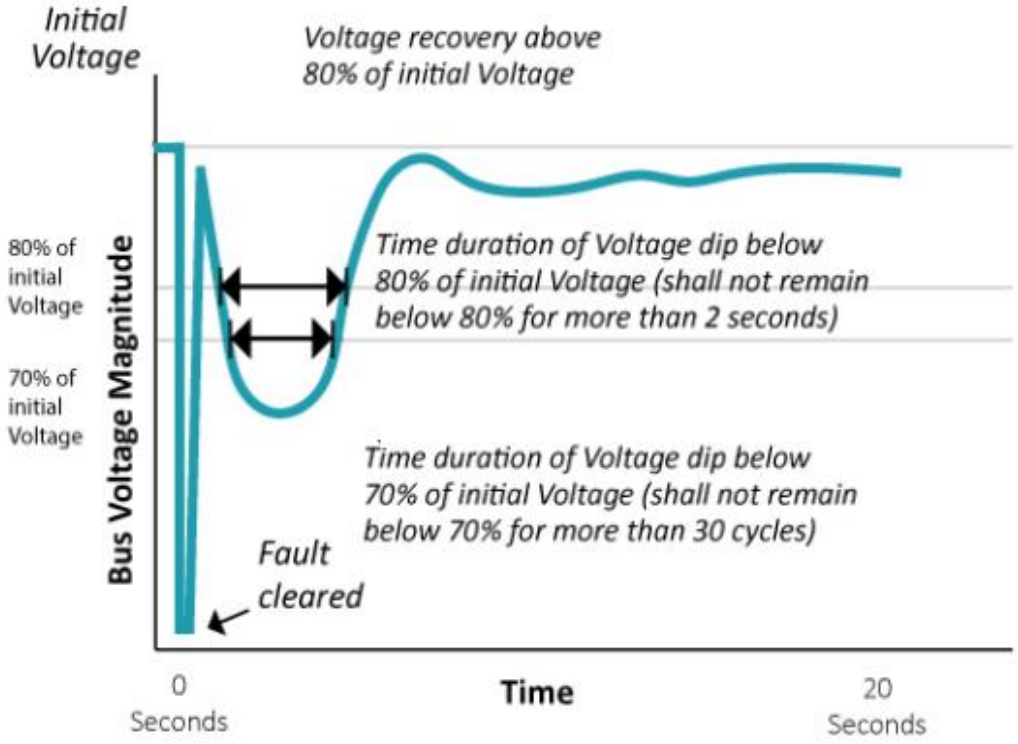

Figure 3.5: WECC 70% and 80% voltage dip criteria [46]

These WECC TPL criteria are always checked before deciding the IRG penetration threshold. Moreover, the stability of the system is also verified to ensure that the system does not collapse post-contingency.

3.3.2 Tie line power flow limits

Another constraint that has to be considered is the tie line limits. When the distribution of generation in an area changes, the export and import of power could change with the neighboring areas [47]. Also, neighboring areas usually have agreement on how much power can be exported or imported through the tie lines. Redispatching the power among the generators is another method that can be applied to optimize the IRG penetration threshold while keeping the tie line power flow under control and not jeopardizing the health of the power grid [48].

SRP requested to check the tie line limits through PSLF in the original power flow file ".sav" by accessing a specific function called "TieLineArea". This function can be accessed by entering "Tabr" in the power flow case. In that table there were 2 tie line limits, one was for the normal condition (Rating MVA1) and the other one is for the contingency/emergency condition (Rating MVA2). There were 119 tie lines found in the area where the case study was conducted. The identified tie lime limits are shown below in Table 3.1. Since the emergency rating for these 119 tie lines were used extensively in this thesis, they have been highlighted in red in Table 3.1.

Table 3.1: The tie line limits identified in the original power flow file ".sav".

From Bus Number	From Bus Name	To Bus Number	To Bus Name	Power	Reactive Power	From Area	To Area	MVA1	MVA2
24002	BUS 1	34042	Nghbr 160	446.74	6.63	42	34	1905	2572
24003	Bus 2	34041	Nghbr 159	340.4	-143.59	42	36	1947	2572
24004	BUS 3	34040	Nghbr 158	673.54	-13.76	42	34	3291	4503
24005	BUS 4	34039	Nghbr 157	98	-8.37	42	32	866	952
24006	BUS 5	34038	Nghbr 156	-13.52	-119.19	42	20	1195	1195
24007	BUS 6	34037	Nghbr 155	568.73	-35.99	42	20	1004	1195
24008	BUS 7	34036	Nghbr 154	-308.47	120.43	42	75	1026	1300
24009	BUS 8	34035	Nghbr 153	2.47	-120.11	42	29	1200	1200
24010	BUS 9	34034	Nghbr 152	-87.95	0.92	42	29	751	853
24011	BUS 10	34033	Nghbr 151	-97.85	23.83	42	29	407	407
24012	BUS 11	34032	Nghbr 150	-96.39	12.49	42	29	407	407
24013	BUS 12	34031	Nghbr 149	58.88	31.4	42	29	406	406

From Bus Number	From Bus Name	To Bus Number	To Bus Name	Power	Reactive Power	From Area	To Area	MVA1	MVA2
24014	BUS 13	34030	Nghbr 148	102.66	-15.28	42	20	402	402
24015	BUS 14	34029	Nghbr 147	21.61	-5.8	42	29	637	637
24016	BUS 15	34028	Nghbr 146	-50.41	-6.22	42	29	334.6	368
24017	BUS 16	34027	Nghbr 145	-4.71	8.93	42	29	286	286
24018	BUS 17	34026	Nghbr 144	-153.37	31.31	42	29	797	797
24019	BUS 18	34025	Nghbr 143	163	27.78	42	29	713	978
24020	BUS 19	34024	Nghbr 142	-13.73	-0.54	42	29	733	806.3
24021	BUS 20	34023	Nghbr 141	-154.58	-19.91	42	29	335	369
24022	BUS 21	34022	Nghbr 140	-27.89	-11.82	42	29	366.5	403.2
24023	BUS 22	34021	Nghbr 139	-59.53	-14.52	42	29	320	320
24024	BUS 23	34020	Nghbr 138	299.49	-126.36	42	29	548	548
24025	BUS 24	34019	Nghbr 137	-250.99	37.25	42	11	270.9	361.3
24026	BUS 25	34018	Nghbr 136	243.42	-8.91	42	29	800	800
24027	BUS 26	34017	Nghbr 135	-27.98	7.21	42	29	167	167

From Bus Number	From Bus Name	To Bus Number	To Bus Name	Power	Reactive Power	From Area	To Area	MVA1	MVA2
24028	BUS 27	34016	Nghbr 134	-13.75	-2.32	42	29	111.5	111.5
24029	BUS 28	34015	Nghbr 133	-45.47	4.67	42	29	90	90
24030	BUS 29	34014	Nghbr 132	47.22	9.15	42	29	120	120
24031	BUS 30	34013	Nghbr 131	28.19	0.37	42	29	153	153
24032	BUS 31	34012	Nghbr 130	28.93	15.18	42	29	120	120
24033	BUS 32	34011	Nghbr 129	-39.04	-7.41	42	29	172	172
24034	BUS 33	34010	Nghbr 128	0	0	42	29	10000	10000
24035	BUS 34	34009	Nghbr 127	-97.38	-19.33	42	32	239	258.1
24036	BUS 35	34008	Nghbr 126	80.5	14.14	42	29	115	115
24037	BUS 36	34007	Nghbr 125	80.5	14.14	42	29	115	115
24038	BUS 37	34006	Nghbr 124	80.5	14.14	42	29	115	115
24039	BUS 38	34005	Nghbr 123	-95.68	-19.19	42	32	239	258.1
24040	BUS 39	34004	Nghbr 122	83.68	13.76	42	29	115	115
24041	BUS 40	34003	Nghbr 121	83.68	13.76	42	29	115	115
24042	BUS 41	34002	Nghbr 120	-184.05	-11.91	42	32	600	896

From Bus Number	From Bus Name	To Bus Number	To Bus Name	Power	Reactive Power	From Area	To Area	MVA1	MVA2
24043	BUS 42	34001	Nghbr 119	853.7	37.4	42	34	2338	2338
24044	BUS 43	34000	Nghbr 118	393.23	12.63	42	29	1905	2572
24045	BUS 44	33999	Nghbr 117	-512.49	-59.92	42	11	1725	2300
24046	BUS 45	33998	Nghbr 116	764.72	168.71	42	32	2579	2598
24047	BUS 46	33997	Nghbr 115	819.8	76.08	42	32	2579	2598
24048	BUS 47	33996	Nghbr 114	-309.07	-15.79	42	29	1033	1033
24049	BUS 48	33995	Nghbr 113	-309.23	-26.08	42	29	1033	1033
24050	BUS 49	33994	Nghbr 112	-258.76	6	42	29	796.7	796.7
24051	BUS 50	33993	Nghbr 111	-258.76	6	42	29	796.7	796.7
24052	BUS 51	33992	Nghbr 110	-214.7	-46.49	42	29	756	756
24053	BUS 52	33991	Nghbr 109	321.38	-18.6	42	29	813	813
24054	BUS 53	33990	Nghbr 108	148.39	54.5	42	11	160	160
24055	BUS 54	33989	Nghbr 107	150.2	30.49	42	11	160	160
24056	BUS 55	33988	Nghbr 106	150.23	-23.39	42	11	161	161
24057	BUS 56	33987	Nghbr 105	65.13	6.81	42	11	70	70

From Bus Number	From Bus Name	To Bus Number	To Bus Name	Power	Reactive Power	From Area	To Area	MVA1	MVA2
24058	BUS 57	33986	Nghbr 104	-0.99	9.89	42	89	70	70
24059	BUS 58	33985	Nghbr 103	109.5	15.59	42	29	120	120
24060	BUS 59	33984	Nghbr 102	-61.58	-44.67	42	21	717	717.1
24061	BUS 60	33983	Nghbr 101	-5	22.69	42	20	925	1110
24062	BUS 61	33982	Nghbr 100	-5	22.69	42	20	845	1014
24063	BUS 62	33981	Nghbr 99	64.31	-15.69	42	20	218	218
24064	BUS 63	33980	Nghbr 98	73.96	-16.63	42	20	300	300
24065	BUS 64	33979	Nghbr 97	175.98	21.09	42	21	939	1313
24066	BUS 65	33978	Nghbr 96	-51.47	-15.77	42	29	80	89.6
24067	BUS 66	33977	Nghbr 95	-46.52	-13.9	42	29	80	89.6
24068	BUS 67	33976	Nghbr 94	-36.59	-13.23	42	29	80	89.6
24069	BUS 68	33975	Nghbr 93	-44.23	-18.65	42	29	75	84
24070	BUS 69	33974	Nghbr 92	-48.39	-23.63	42	29	75	84
24071	BUS 70	33973	Nghbr 91	-30.77	-11.94	42	29	40	44.8
24072	BUS 71	33972	Nghbr 90	-29.38	-11.4	42	29	40	44.8
24073	BUS 72	33971	Nghbr 89	-36.59	-13.23	42	29	80	89.6

From Bus Number	From Bus Name	To Bus Number	To Bus Name	Power	Reactive Power	From Area	To Area	MVA1	MVA2
24074	BUS 73	33970	Nghbr 88	0	0.1	42	29	200	224
24075	BUS 74	33969	Nghbr 87	-0.04	-0.23	42	29	80	89
24076	BUS 75	33968	Nghbr 86	-0.04	-0.23	42	29	80	89
24077	BUS 76	33967	Nghbr 85	-1.01	-0.24	42	29	100	110
24078	BUS 77	33966	Nghbr 84	-9.3	-2.98	42	29	450	495
24079	BUS 78	33965	Nghbr 83	1.39	-0.45	42	20	20	20
24080	BUS 79	33964	Nghbr 82	77.38	-3.69	42	29	171.1	217.3
24081	BUS 80	33963	Nghbr 81	-65.54	1.45	42	29	143	159
24082	BUS 81	33962	Nghbr 80	-16.5	0.86	42	29	235	306
24083	BUS 82	33961	Nghbr 79	-139.08	-33.99	42	29	471	478
24084	BUS 83	33960	Nghbr 78	-14.01	-1.49	42	29	112	140
24085	BUS 84	33959	Nghbr 77	-13.09	-4.01	42	29	100	112
24086	BUS 85	33958	Nghbr 76	-43.3	0	42	29	334	350
24087	BUS 86	33957	Nghbr 75	-10.7	-0.01	42	29	120	132
24088	BUS 87	33956	Nghbr 74	-13.51	-0.01	42	29	120	132

From Bus Number	From Bus Name	To Bus Number	To Bus Name	Power	Reactive Power	From Area	To Area	MVA1	MVA2
24089	BUS 88	33955	Nghbr 73	-10.19	-0.01	42	29	120	140
24090	BUS 89	33954	Nghbr 72	-3.3	0	42	29	120	132
24091	BUS 90	33953	Nghbr 71	-3.1	0	42	29	120	132
24092	BUS 91	33952	Nghbr 70	-6.5	0	42	29	120	132
24093	BUS 92	33951	Nghbr 69	-2.4	0.01	42	29	120	132
24094	BUS 93	33950	Nghbr 68	-3.3	0	42	29	120	132
24095	BUS 94	33949	Nghbr 67	-2.8	0	42	29	120	140
24096	BUS 95	33948	Nghbr 66	-48	0	42	29	150	150
24097	BUS 96	33947	Nghbr 65	-48	0	42	29	150	150
24098	BUS 97	33946	Nghbr 64	-48	0	42	29	150	150
24099	BUS 98	33945	Nghbr 63	14	5.89	42	29	70	70
24100	BUS 99	33944	Nghbr 62	14	5.89	42	29	70	70
24101	BUS 100	33943	Nghbr 61	-32.2	-6.53	42	29	100	110
24102	BUS 101	33942	Nghbr 60	3.26	2.48	42	29	119	147
24103	BUS 102	33941	Nghbr 59	-24.81	-5.02	42	29	120	120
24104	BUS 103	33940	Nghbr 58	-13.64	-2.83	42	29	50	62.5

From Bus Number	From Bus Name	To Bus Number	To Bus Name	Power	Reactive Power	From Area	To Area	MVA1	MVA2
24105	BUS 104	33939	Nghbr 57	-11.47	-0.32	42	29	135	150
24106	BUS 105	33938	Nghbr 56	0	0	42	29	37	37
24107	BUS 106	33937	Nghbr 55	-4.63	-0.21	42	29	191	191
24108	BUS 107	33936	Nghbr 54	1.8	0.59	42	29	100	100
24109	BUS 108	33935	Nghbr 53	51.27	-3.8	42	29	197	197
24110	BUS 109	33934	Nghbr 52	7.49	7.9	42	31	73	73
24111	BUS 110	33933	Nghbr 51	6.71	-14.93	42	31	75	82.5
24112	BUS 111	33932	Nghbr 50	-41.78	-35.54	42	31	98	98
24113	BUS 112	33931	Nghbr 49	-87.13	-48.92	42	29	191	191
24114	BUS 113	33930	Nghbr 48	14.98	-4.73	42	29	191.5	191.5
24115	BUS 114	33929	Nghbr 47	5.9	4.37	42	29	20	22
24116	BUS 115	33928	Nghbr 46	-6.81	-1.39	42	29	20	20
24117	BUS 116	33927	Nghbr 45	0	0	42	29	7.5	7.5
24118	BUS 117	33926	Nghbr 44	0	0	42	29	7.5	7.5

From Bus Number	From Bus Name	To Bus Number	To Bus Name	Power	Reactive Power	From Area	To Area	MVA1	MVA2
24119	BUS 118	33925	Nghbr 43	250.52	33.86	42	32	1028	1028
24120	BUS 119	33924	Nghbr 42	28.83	-14.48	42	29	135.1	143.8

After identifying the tie line limits, the power flow through these lines needed to be monitored. A model called "imetr" in the dynamic file ".dyd" that records branch current was used to record the real power, reactive power, current, branch loading and branch current. This model was added to all the identified tie lines connecting the area-under-study with its neighboring areas. Transformers which were on the border between the areas were included in the analysis too. The EPCL scripts ".p" through PSLF PLOT that extracted the real and reactive powers can be found in Appendices A & B.

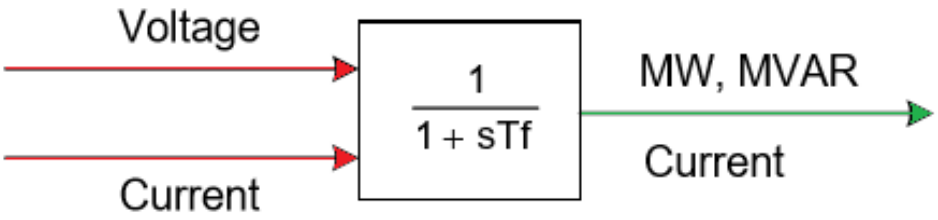

Figure 3.6: "imetr" model block diagram

3.4 Step 4: Create an EPCL script ".p" to process the output channel files to check the performance and detect any violations of the standards (post-simulation)

In this step, the output of simulation has to analyzed and checked to see if it fits the criteria and if it is reliable to continue the case study on it. Another accompanying program with PSLF called PLOT21 was used to access the generated data files for the models in order to visualize them as graphs. This program can also be used to analyze the graphs and draw inferences. An EPCL code was created to check the WECC TPL criteria to match the output of the simulations. This script is anonymous due to copyright.

3.5 Step 5: Create a Python script ".py" to check if the power flow in the tie lines between areas are exceeding the limits (post-simulation)

After obtaining tie line power flow information in Step 3, there has to be a script to check if the system exceeds these power flows. A Python script was created to utilize the tie line power flow limits in the contingency case (MVA2) in Table 3. 1. The Python script can be seen in Appendix C. Tie line power flow was not mentioned in the WECC TPL criteria but noted by SRP as one aspect they look at when conducting expansion planning.

3.6 Step 6: Run the EPCL script through PSLF with the associated contingency list and the post-simulation scripts to check for any violations

After readying all the scripts for analyzing the output data from simulations, the original case can be tested and simulated starting from Step 6. It was noted that the IRG penetration in the original system was 11%, and natural gas was responsible for most of the power generation as shown in Fig. 3.7.

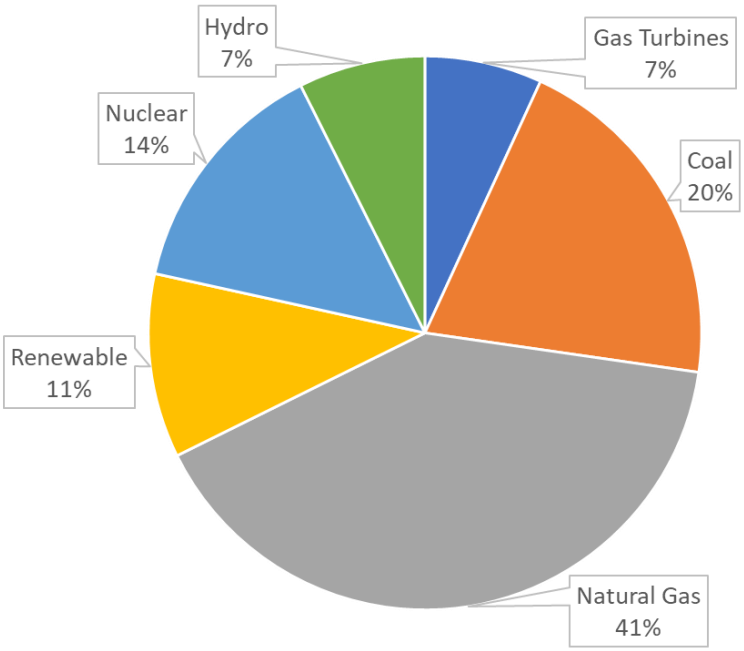

Figure 3.7: Power generation distribution in the original case

All the 56 contingency cases were run smoothly using the EPCL script ".p" and with the associated switch files for each contingency ".swt" case. However, 4 contingency

cases violated WECC TPL criteria. Table 3.2 below shows the performance of the cases, with the cells highlighted in red representing the cases with violations.

Table 3.2: Original case performance considering the WECC TPL criteria and tie line limits

Contingency Cases	MVA Exceeded	Voltage Violations	Frequency Violations
Generator Contingency Case 1	17.23	0	0
Generator Contingency Case 2	21.24	0	1
Generator Contingency Case 3	0	0	0
Generator Contingency Case 4	2.33	0	4
Generator Contingency Case 5	30.78	0	0
Generator Contingency Case 6	0	0	1
Generator Contingency Case 7	3.08	0	0
Generator Contingency Case 8	8.7	0	0
Line Fault Contingency 1	3.7	0	0
Line Fault Contingency 2	5.95	0	0
Line Fault Contingency 3	24	0	0
Line Fault Contingency 4	15.23	0	0
Line Fault Contingency 5	55.3	0	0
Line Fault Contingency 6	52.3	0	0
Line Fault Contingency 7	16	0	0
Line Fault Contingency 8	35.2	0	0
Line Fault Contingency 9	35.3	0	0
Line Fault Contingency 10	35.3	0	0

Contingency Cases	MVA Exceeded	Voltage Violations	Frequency Violations
Line Fault Contingency 11	35.5	0	0
Line Fault Contingency 12	15.31	0	0
Line Fault Contingency 13	20.6	0	0
Line Fault Contingency 14	54.7	0	0
Line Fault Contingency 15	17.9	0	0
Line Fault Contingency 16	21.6	0	0
Line Fault Contingency 17	23.4	0	0
Line Fault Contingency 18	56.7	0	0
Line Fault Contingency 19	11.7	0	0
Line Fault Contingency 20	21.5	0	0
Line Fault Contingency 21	30.8	0	0
Line Fault Contingency 22	23.4	0	0
Line Fault Contingency 23	0	0	0
Line Fault Contingency 24	51.8	0	0
Line Fault Contingency 25	0	0	0
Line Fault Contingency 26	31.3	0	0
Line Fault Contingency 27	47.6	0	0
Line Fault Contingency 28	0	0	0
Line Fault Contingency 29	0	0	0
Line Fault Contingency 30	0	0	0
Line Fault Contingency 31	4.8	0	0
Line Fault Contingency 32	0	0	0

Contingency Cases	MVA Exceeded	Voltage Violations	Frequency Violations
Line Fault Contingency 33	51.6	0	0
Line Fault Contingency 34	40.6	0	0
Line Fault Contingency 35	0	0	0
Line Fault Contingency 36	0	0	0
Line Fault Contingency 37	32.2	0	0
Line Fault Contingency 38	31.3	0	0
Line Fault Contingency 39	40.3	0	0
Line Fault Contingency 40	40.3	0	0
Line Fault Contingency 41	32	0	1
Line Fault Contingency 42	34.5	0	0
Line Fault Contingency 43	55.13	0	0
Line Fault Contingency 44	17.2	0	0
Line Fault Contingency 45	8.2	0	0
Line Fault Contingency 46	8.4	0	0
Line Fault Contingency 47	5.8	0	0
Line Fault Contingency 48	47.3	0	0

The frequency violations occurred in Line Fault Contingency 41 is caused because of a radial line in the system that has slower frequency recovery and was a reasonable reaction. The WECC TPL criteria that was violated in that case was the 59.6 Hz frequency deviation criteria, where the frequency at that bus remained below 59.6 Hz for more than 6 cycles but recovered after that as shown in Figure 3.8 below.

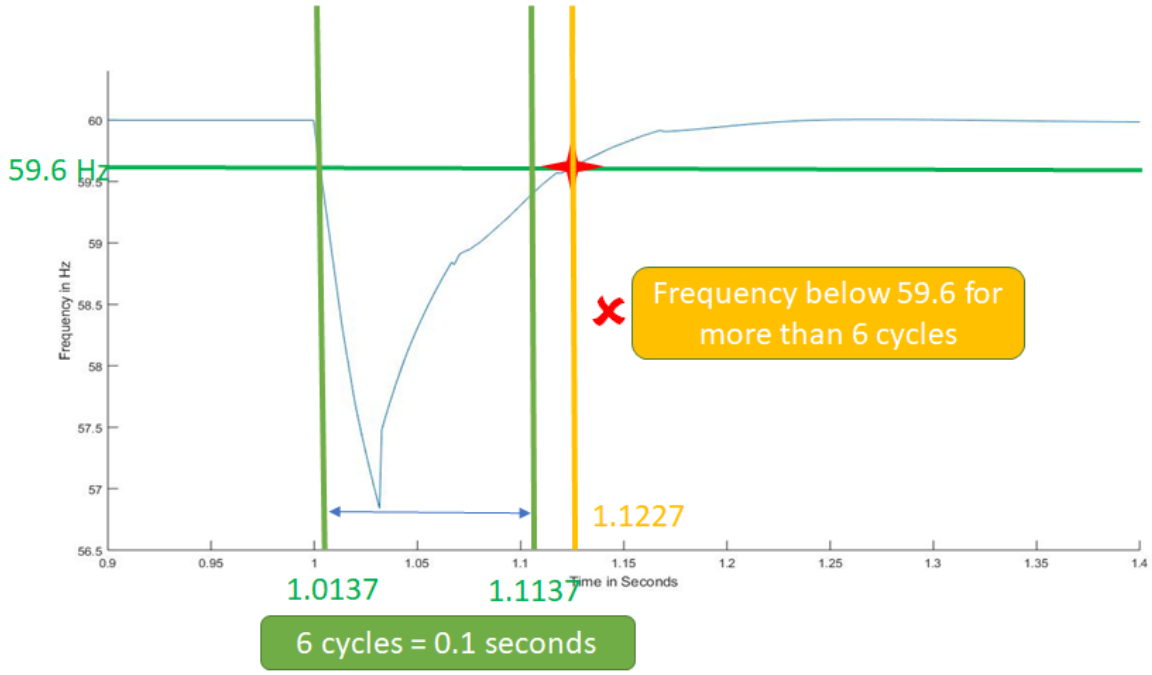

Figure 3.8: Line fault contingency 41 where frequency remained less than 59.6 for more than 6 cycles (0.1 seconds)

In order to verify that the bus is located at a radial line, scan function in PSLF was used to access the circuit schematic of the bus with violation. Fig. 3.9 shows the radial connection.

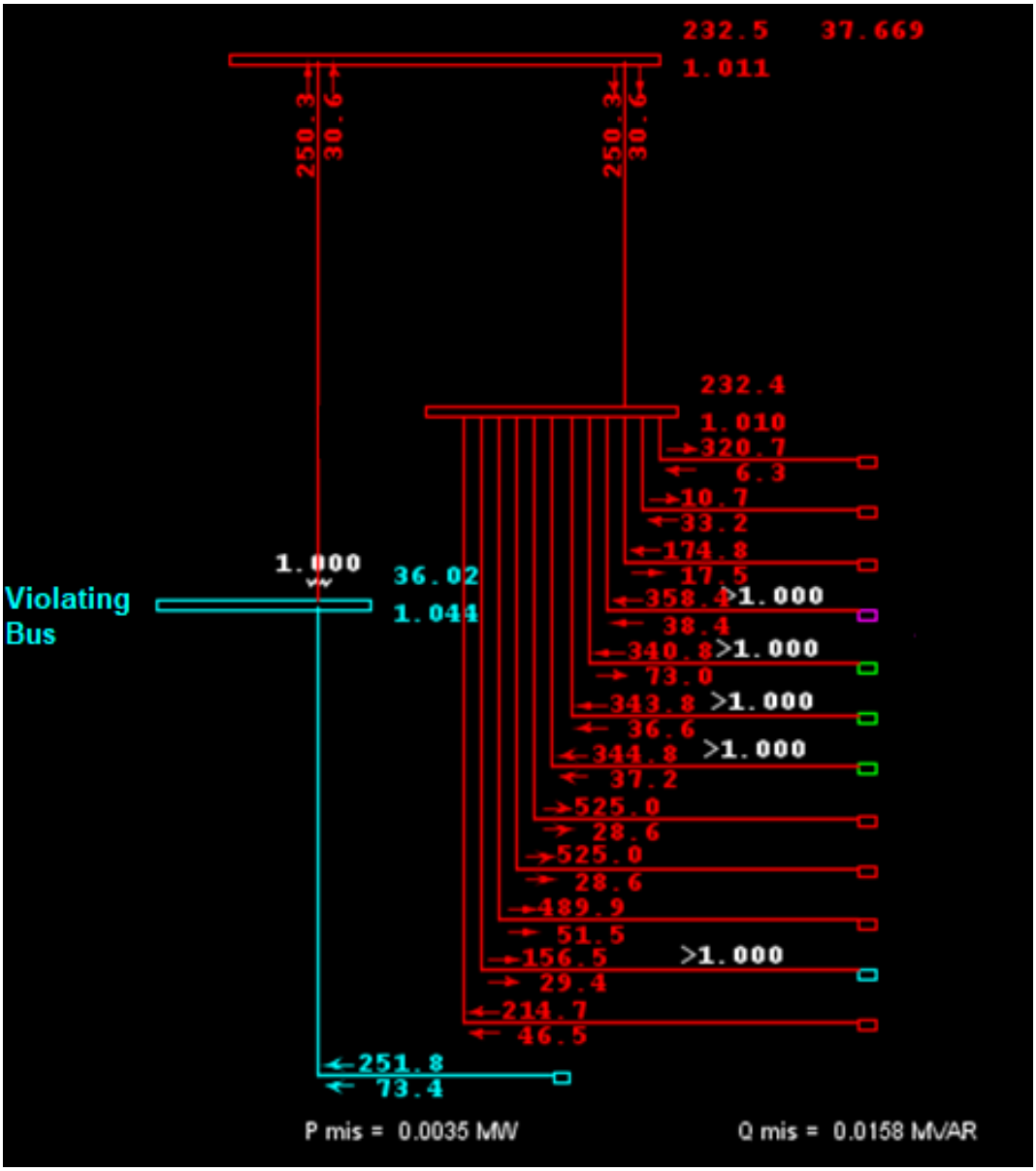

Figure 3.9: Violating bus at a radial line

The other violations in the original case occurred at 3 generator contingencies. The switch file for Generator Contingency Case 4 had to be reviewed to check the scenarios in it. The switch file for the Generator Contingency 4 included the following actions explained below:

Actions in switch file (.swt):

- At 0+ Second
    1. Trip Generator GEN 87S (148 MW)
    2. Modify Bus Load GEN 87A
- At 1 second
    1. Fault Bus GENGT
- At 1.1 Second
    1. Clear Faulted Bus GENGT
    2. Trip Generator GEN 87S (106 MW)
    3. Modify Bus Load GEN 87S

Violations:

The frequency at the following buses remained below 59.6 Hz for more than 6 cycles (0.1 seconds):

1. BUS11 17349
2. BUS12 17347
3. BUS13 17355
4. BUS14 17345

Fig. 3.10 shows the frequency behavior of these four buses.

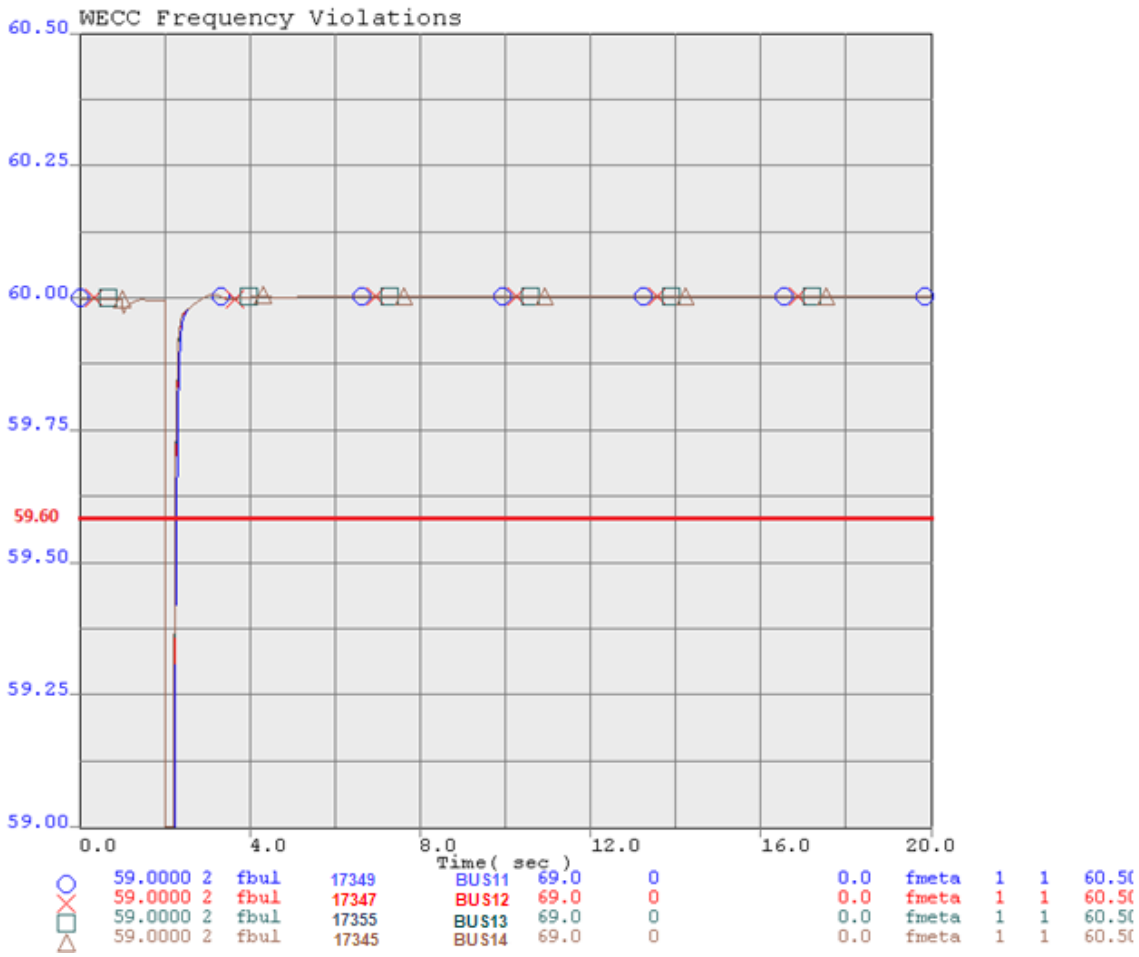

Figure 3.10: The frequency violations in Generator Contingency Case 4

Furthermore, some contingency cases had the tie line limits exceed within reasonable amounts. Therefore, the goal for the next step when the IRG penetration was modified was to not exceed the amount of MVA that was exceeded in the original case. The results were shown to SRP engineers, and they agreed with this rationale. Finally, note that the methodology does not seek to enhance the original case in terms of the amount of violations or tie line power flow, but to analyze the original case in order to compare it

with the next step where IRG penetration is increased and ensure that the system is not worse.

3.7 Step 7: Identify the generation units that can be removed from the system and replaced with IRG units

The current trend of going towards "clean energy" is to not only add more renewable energy in the power grid, but also to shut down the most polluted source of energy in the system and replace them with the newly proposed renewable generation units. Therefore, identifying the synchronous generators in the system is essential before adding any IRG units into the system. Coal-fired and gas-turbine unites were identified in the system for this purpose, which had a total capacity of 7,384 MW.

After adding the newly proposed IRG units in the (gens) table in the edit function of PSLF, the bus type where the IRG was added was changed from PQ (load bus) to PV (generator bus). The bus type can be changed in the (bus) table in PSLF. After doing so, the system was re-solved to check for converge with a mismatch which equals or is less than 0.1 MW and 0.9 MVAR for real power and reactive power, respectively. For the dynamic file ".dyd", the removed conventional units' models in the dynamic file were removed as well. For the newly added IRG units, (regc_a) model shown in Fig. 3.11 was used to simulate a renewable generator, while a (reec_a) controller model shown in Fig 3.12 and (reec_b) controller model shown in Fig 3.13 were used for solar PV and battery storage, respectively.

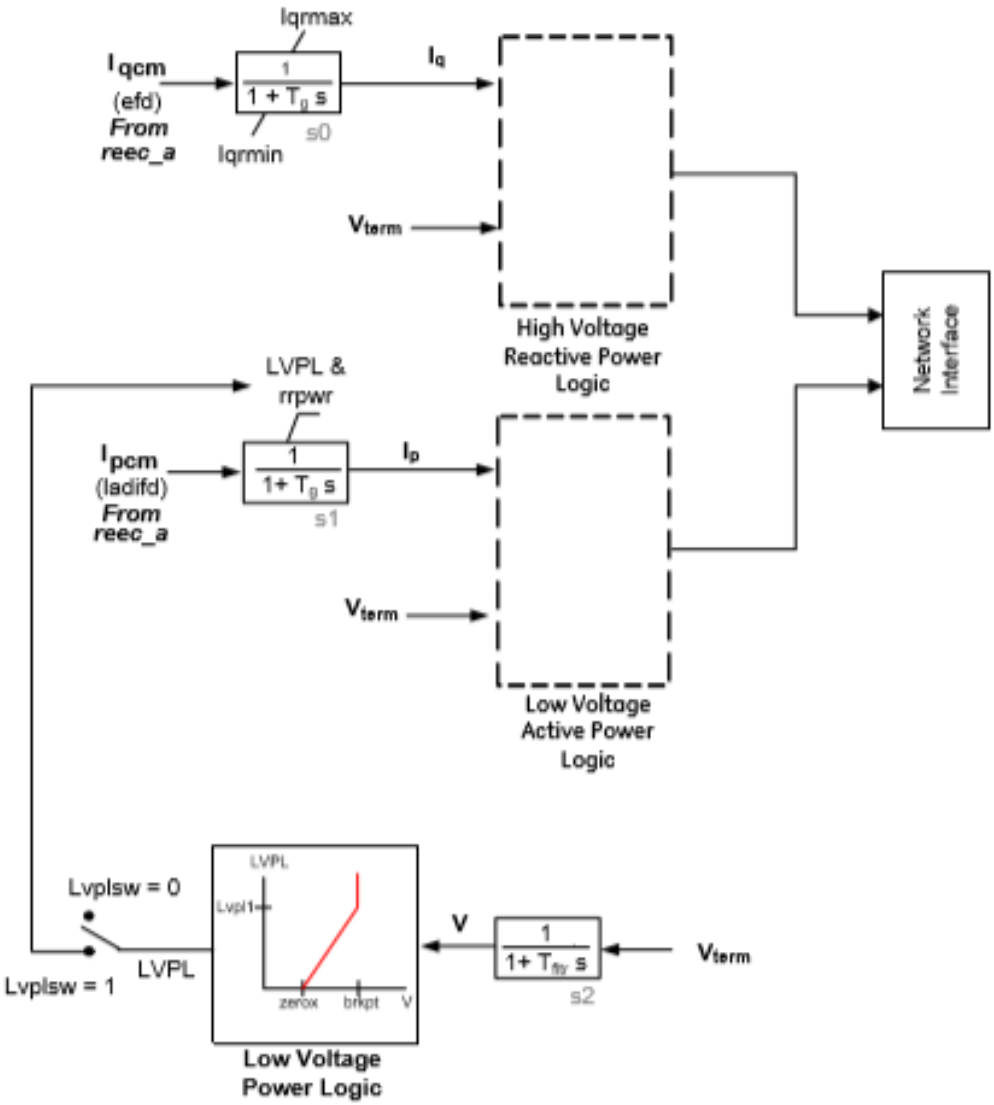

Figure 3.11: (regc_a) model block diagram

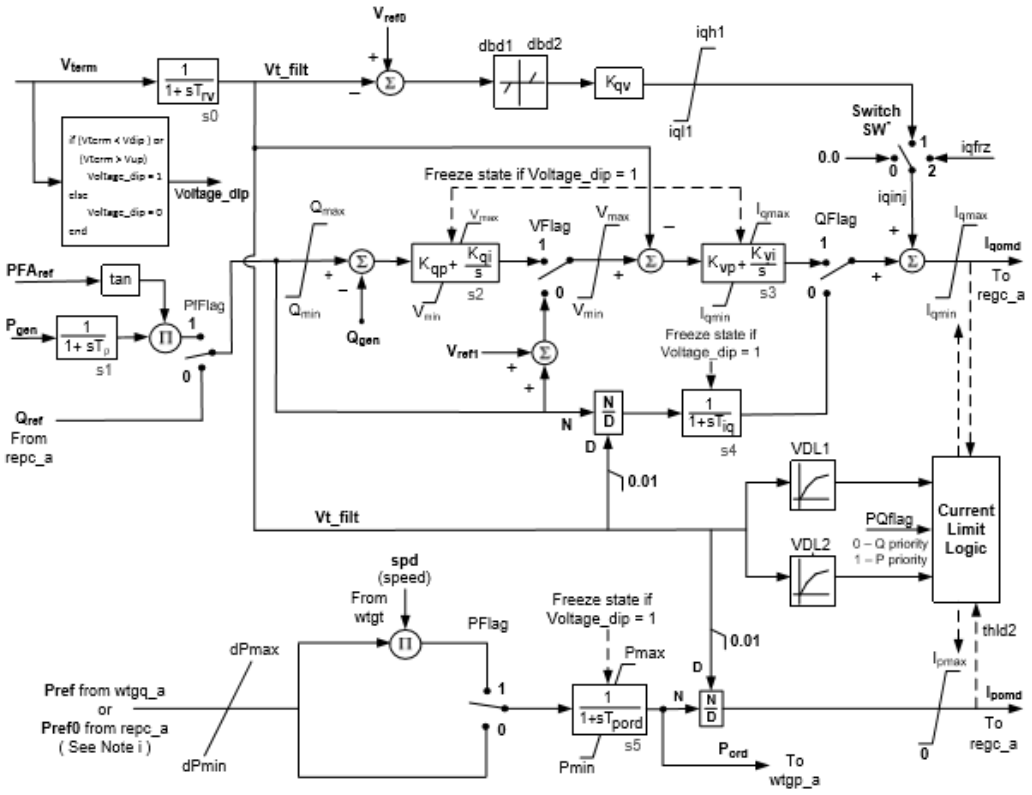

Figure 3.12: (reec_a) block diagram

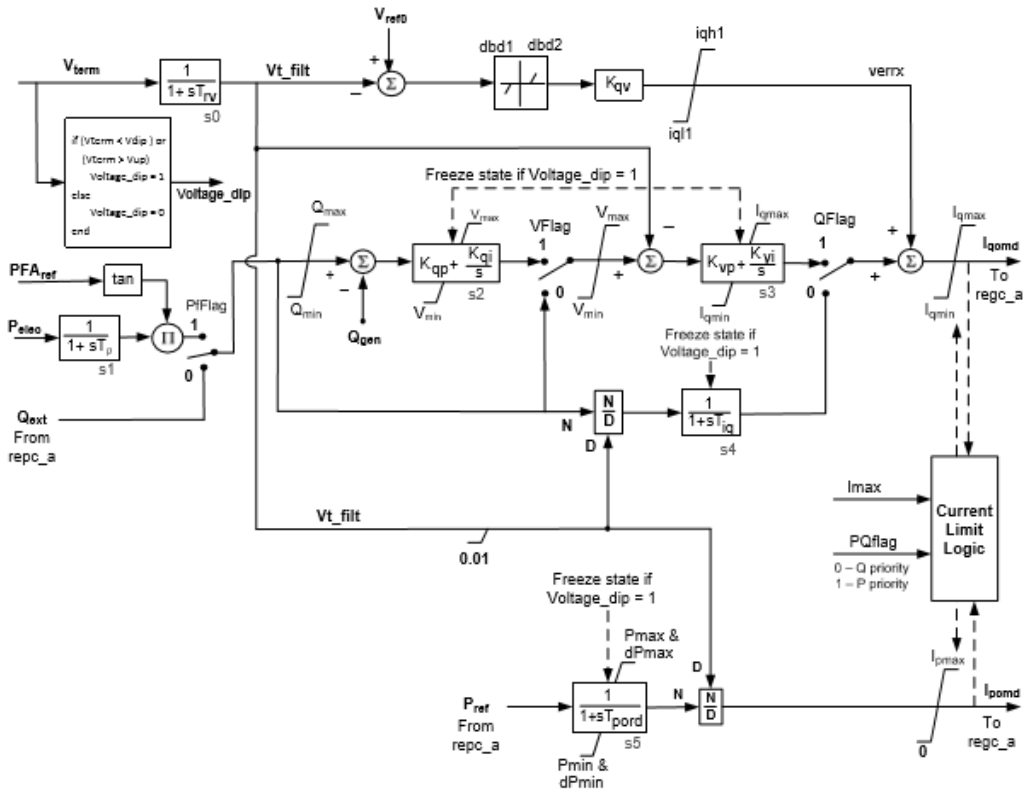

Figure 3.13: (reec_b) block diagram

The coal-fired and gas turbine units were shut down and IRG units were added in place but in different locations in the system as requested by SRP for this case study. On doing so, the IRG penetration increased from 11% to 41% as shown in Fig. 3.14 below.

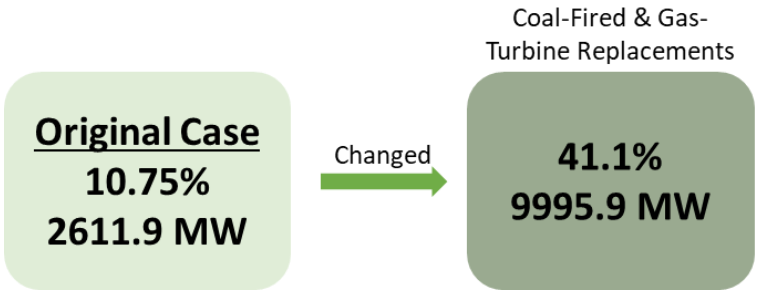

Figure 3.14: IRG penetration increase after exhausting all coal-fired and gas-turbine units in the case study

3.8 Step 8: Run the EPCL script through PSLF with the associated contingency lists and post-simulation scripts to check for any violations

After completing Step 7, the system had a very high IRG penetration. Therefore, the case was run through the WECC TPL EPCL script ".p" and the tie line power flow limits analyzer Python code ".p". Table 3.3 and Fig. 3.15 show the performance of the 41% IRG case.

Table 3.3: High IRG penetration case (41%) performance considering the WECC TPL criteria and tie line limits

Contingency Cases	Total MVA Exceeded	Voltage Violations	Frequency Violations
Generator Contingency Case 1	0	0	0
Generator Contingency Case 2	50.23	0	1
Generator Contingency Case 3	38.13	0	0
Generator Contingency Case 4	22.78	0	4
Generator Contingency Case 5	42.75	0	0
Generator Contingency Case 6	0	0	1
Generator Contingency Case 7	13.46	0	0
Generator Contingency Case 8	22.3	0	0
Line Fault Contingency 1	26.21	0	0
Line Fault Contingency 2	28.3	0	0
Line Fault Contingency 3	37.51	0	0
Line Fault Contingency 4	26.56	0	0

Contingency Cases	Total MVA Exceeded	Voltage Violations	Frequency Violations
Line Fault Contingency 5	65.5	0	0
Line Fault Contingency 6	62.05	0	0
Line Fault Contingency 7	32.34	0	0
Line Fault Contingency 8	54.16	0	0
Line Fault Contingency 9	53.96	0	0
Line Fault Contingency 10	54.11	0	0
Line Fault Contingency 11	54.11	0	0
Line Fault Contingency 12	37.56	0	0
Line Fault Contingency 13	34.71	0	0
Line Fault Contingency 14	57.25	0	0
Line Fault Contingency 15	34.3	0	0
Line Fault Contingency 16	33.6	0	0
Line Fault Contingency 17	36.8	0	0
Line Fault Contingency 18	61.76	0	0
Line Fault Contingency 19	20.97	0	0
Line Fault Contingency 20	33.34	0	0
Line Fault Contingency 21	36.9	0	0
Line Fault Contingency 22	36.6	0	0
Line Fault Contingency 23	0	0	0
Line Fault Contingency 24	58.9	0	0

Contingency Cases	Total MVA Exceeded	Voltage Violations	Frequency Violations
Line Fault Contingency 25	0	0	0
Line Fault Contingency 26	59.4	0	0
Line Fault Contingency 27	58.9	0	0
Line Fault Contingency 28	0	0	0
Line Fault Contingency 29	0	0	0
Line Fault Contingency 30	0	0	0
Line Fault Contingency 31	49.48	0	0
Line Fault Contingency 32	0	0	0
Line Fault Contingency 33	58.97	0	0
Line Fault Contingency 34	59.01	0	0
Line Fault Contingency 35	0	0	0
Line Fault Contingency 36	0	0	0
Line Fault Contingency 37	45.6	0	0
Line Fault Contingency 38	45.42	0	0
Line Fault Contingency 39	55.45	0	0
Line Fault Contingency 40	55.45	0	0
Line Fault Contingency 41	42.1	0	1
Line Fault Contingency 42	56.6	0	0
Line Fault Contingency 43	65.6	0	0
Line Fault Contingency 44	33.5	0	0

Contingency Cases	Total MVA Exceeded	Voltage Violations	Frequency Violations
Line Fault Contingency 45	29.8	0	0
Line Fault Contingency 46	18.8	0	0
Line Fault Contingency 47	28.4	0	0
Line Fault Contingency 48	67.8	0	0

It is noticeable that there are no extra violations of WECC TPL criteria (the cells highlighted in red are the same for both Tables 3.2 and 3.3). However, there is a significant increase of MVA flow over the original case in the tie lines. Fig. 3.15 shows how the 41% IRG Case compared to the original case (that had 11% IRG).

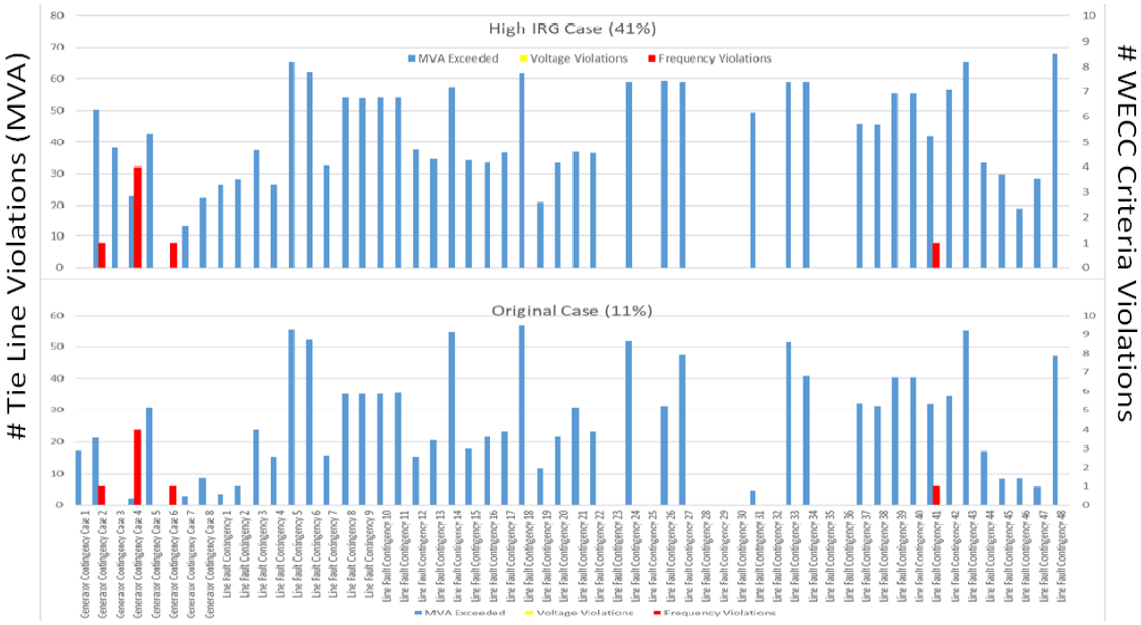

Figure 3.15: The graph charts show how the high IRG case (41%) compared to the original case (11%) has violated tie line limits more significantly

From Fig. 3.15 it becomes clear that the tie line limits are exceeded to a much higher extent than the original case. Thus, the high IRG case (41%) had to be reduced and adjusted accordingly and to do so the Power flow ".sav" and dynamic file ".dyd" were re-modified to create a newer case by following Step 7.

Iterations were performed between Steps 7 and 8 until a reasonable amount of MVA exceeded compared to the original was reached. The IRG penetration dropped significantly to 28%. Fig. 3.16 shows how the 28% IRG case performs in comparison to the original case (which had 11% IRG).

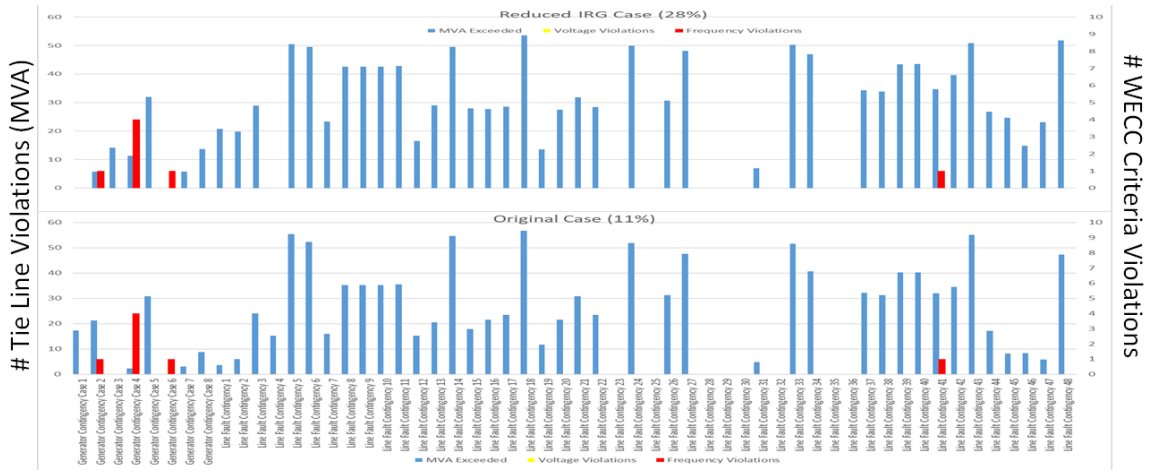

Figure 3.16: The graph charts show how the reduced IRG case (28%) compared to the original case (11%) has a similar pattern of MVA exceeding the tie line limits

From Fig. 3.16, it is clear that the IRG penetration of 28% has reasonable performance in comparison to the original case, which qualifies the study to go to Phase 2 where the system's ability to handle different sensitivity scenarios was investigated.

CHAPTER 4

PENETRATION THRESHOLD OF IRG WITH RESPECT TO DIFFERENT SENSITIVITIES

The IRG penetration threshold must be analyzed for its reliability and stability with different cases that utilities can consider based on NERC studies and WECC expected future criteria. Momentary cessation due to low voltages, modeling the transmission connected solar-based generation compared to the distribution connected solar-based generation, and stalling of induction motors are three sensitivities mentioned in NERC studies that appear to have significant effect on power system operation. The effects of these three sensitivities on the IRG penetration threshold computed for the given test system in the previous chapter are analyzed below.

4.1 Momentary Cessation

Momentary cessation is one of the criteria that NERC is researching and has proposed to WECC to consider in their criteria of stability. This need arose due to a disturbance event of a wildfire in California on Aug 16, 2016, where the fire caused interruption of solar PV generation in the transmission corridor [49]. After investigating that event, NERC recommended utilities to model momentary cessation of inverters in the planning phase to understand how the system behaves if such a scenario manifests again in the future [49]. As such, momentary cessation is an important criterion that must be considered when planning for IRG penetration in the grid.

The modeling of momentary cessation was done by relaxing the "zerox", which is a parameter in the renewable generator models (regc_a). This parameter enables the momentary cessation mode once the voltage goes below it. As such, momentary cessation will occur as many times as the voltages of the IRG go below the threshold specified for them.

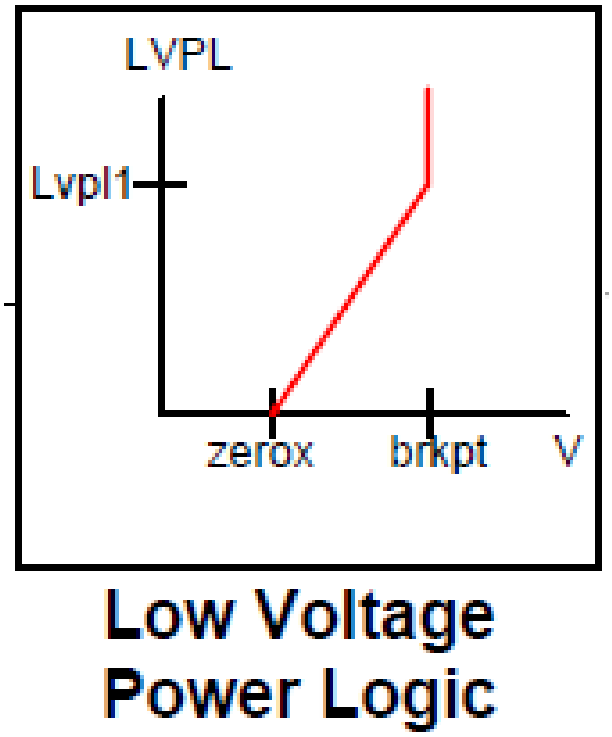

Figure 4.1: A graph that shows the logic of "lvlp" parameter in (regc_a) model

Functionality of the "lvpl1" parameter in (regc_a) model as shown in Fig. 4.1 above is as follows:

- If voltage is greater than the "brkpt", no limit is applied to real power command
- If voltage is between "brkpt" and "zerox", "Lvpl1" is used to calculate the limit for the real power command

- If voltage is less than or equal to “zerox”, real power command is zero (“momentary cessation” mode)
- The ramp rate during voltage recovery is determined by the “rrpwr” value. When “rrpwr” is set to 1 it implies 100% voltage recovery in 1 second

Fig. 4.2 shows the parameters values matched with the “lvpl1” parameter logic graph, while Fig. 4.3 shows how the system operates when it has a high value of “zerox”. It can be seen from Fig. 4.3 that power generation drops to zero once the voltage goes below the “zerox” parameter.

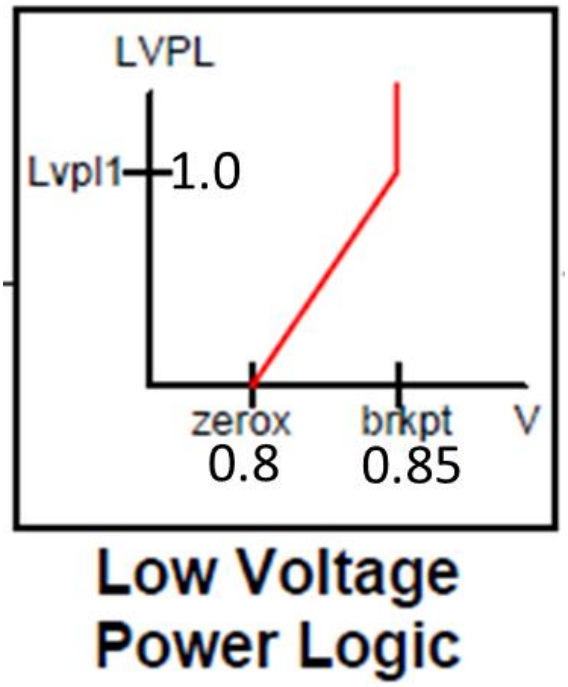

Figure 4.2: A graph shows (regc_a) model parameters with high momentary cessation sensitivity

Figure 4.3: The performance of power generation the unit shown in Fig 4.2 above, notice the power generation drops to 0 when the voltage goes below 0.85

The parameter “zerox” was relaxed to 0.4 p.u. as SRP requested for all the newly add IRG units in the case study. After these adjustments were made in the dynamic file “.dyd”, the 56 contingency list were simulated and the results compared to the original case, as shown in Fig. 4.4.

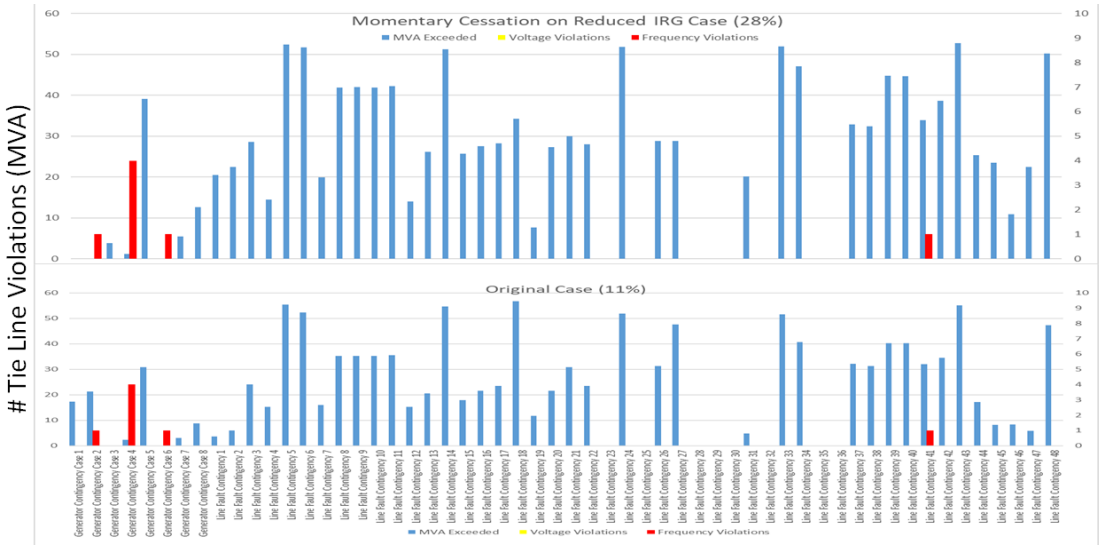

Figure 4.4: Comparison for the performance of the original case and the 28% IRG case with relaxed "zerox" for modeling momentary cessation

From Fig. 4.4, it is clear that enabling momentary cessation has not deteriorated the system performance in any way. Therefore, momentary cessation was found to be a non-binding constraint for the conducted case study and the IRG penetration threshold was kept at 28%.

4.2 Transmission connected solar-based generation VS. Distribution connected Solar-based generation

Another sensitivity study that is valuable for utilities is the difference in the performance of the system when there is transmission connected solar-based generation versus distribution connected solar-based generation [50]. This sensitivity analysis can help utilities understand how their system will perform when there is large number of roof-top solar PV generation coming in from the distribution system instead of a solar farm that can be more directly monitored by the utility.

The (regc_a) model, by default, corresponds to the transmission connected solar-based generation. To model the distribution connected solar-based generation, the (regc_a) model was swapped with the distribution model (pvd1), as shown in Fig. 4.5 below. Fig. 4.6 compares the performance of the test system when the distribution connected solar-based generation replaced the newly added IRG units in Chapter 3.

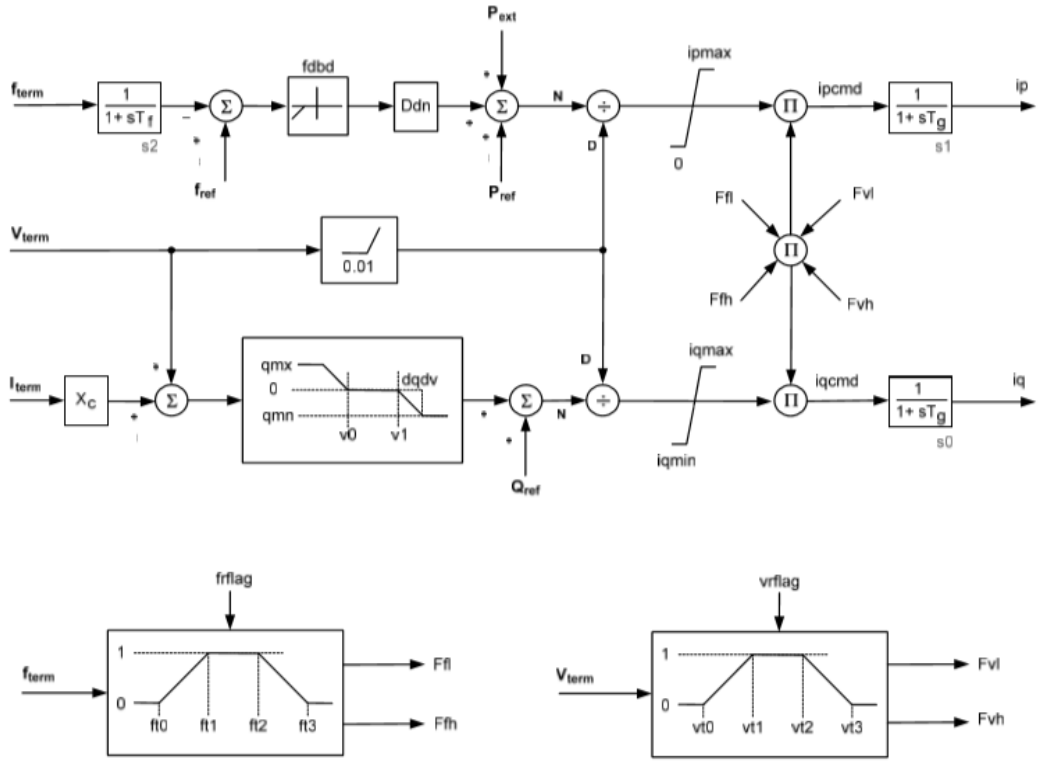

Figure 4.5: (pvd1) model block diagram

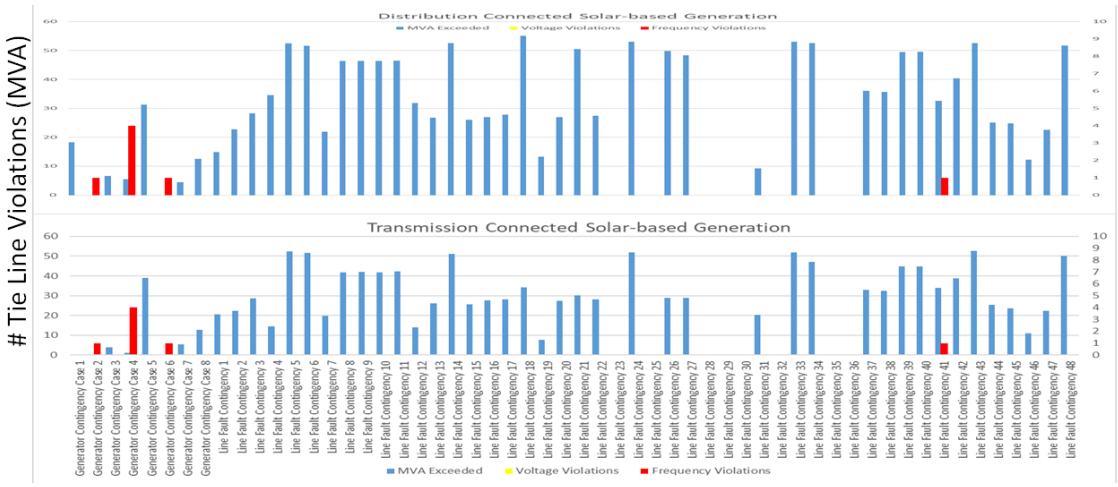

Figure 4.6: Comparison on how similar the Solar vs. Distribution is connected solar based models' performances

From Fig. 4.6 it is realized that the system survived 52 contingencies except the 4 contingencies that violated the standards in the original case (transmission connected solar-based generation). There was a slight increase in MVA of tie-line flows (in the range of 5-20 MVA), but they were considered to be reasonable by SRP engineers. Accordingly, the IRG penetration threshold was not adjusted and it remained at 28%.

4.3 Stalling of induction motors

The last sensitivity to be considered in this methodology is stalling of induction motors. This modeling imitates the stalling of single-phase air conditioner motors due to low voltages. This sensitivity study involved modifying all the composite load models (cmpldw) of the system. The first parameter that was changed in the dynamic file ".dyd" was the stall delay time "tstall"; it was changed from 0.6 p.u. to 0.42 p.u. Next, stalling threshold voltage was enabled. It was changed from 9999.0 p.u. to 0.033 p.u. as mandated

by NERC [51]. There were about 800 models in the test system, all of which were modified to correctly model the stalling of induction motors.

After completing the needed modifications, the case study was run to check its performance with regards to the WECC TPL criteria and the tie-line limits. It was noticed that the case generated many voltage violations in many contingency cases. Therefore, the original case was tested with the stalling of induction motors to check whether it was a problem in the system already or a new problem that needed to be addressed.

Fig. 4.7 and Fig 4.8 below shows that stalling of inductions motors in the original case also generated many voltage violations, but they were not as many or as high as the 28% IRG penetration case. For example, for some of the contingency cases, the violations are 30-50 more in number, than the corresponding contingency of the original case. Therefore, the IRG penetration was readjusted to ensure that the violations did not get worse. Iterating between different combinations of power distributions resulted in an IRG penetration threshold of 15% as shown in Fig. 4.9 below. Moreover, for a clearer comparison on the effect of procedures and results of this methodology on the IRG penetration, Fig. 4.10 shows how the IRG penetration in the case under-study changes throughout Phase 1 and Phase 2.

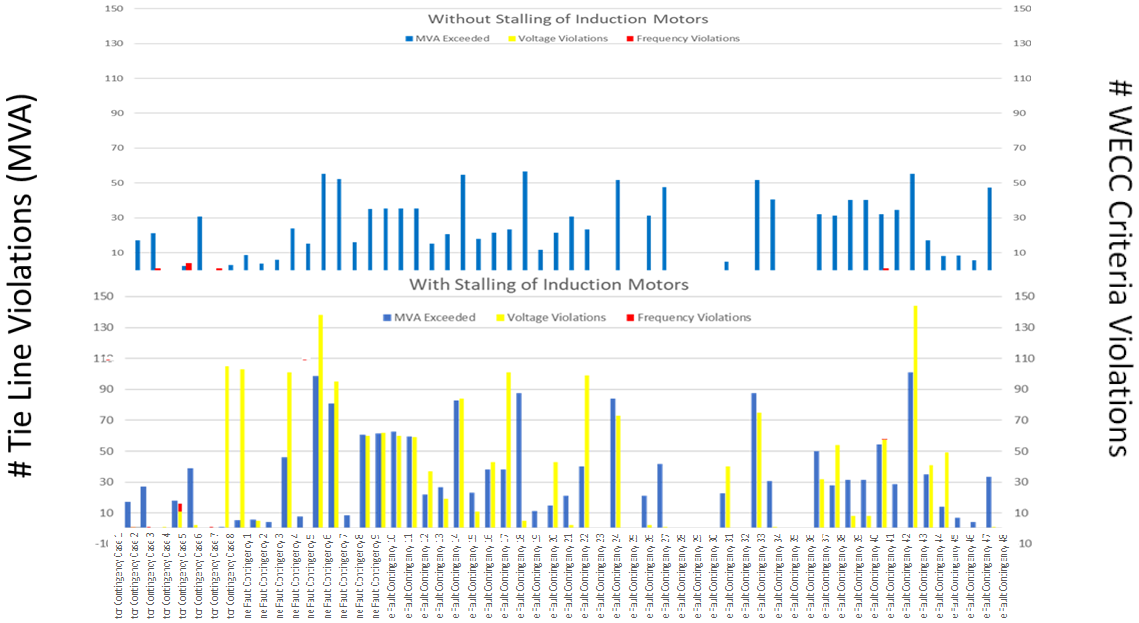

Figure 4.7: Shows how the original case performance changes significantly after applying the stalling of induction motors

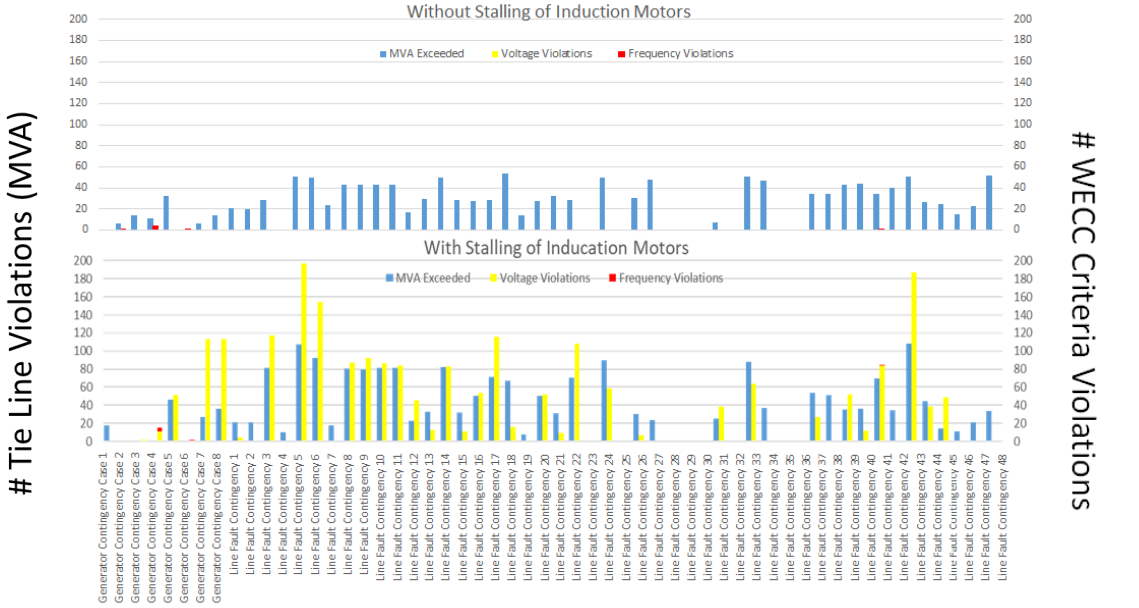

Figure 4.8: Shows how the 28% IRG penetration case's performance changes significantly after applying the stalling of induction motors

Stalling of induction motors was found to be a limiting factor that lowered the IRG penetration threshold dramatically for the system under study. The 15% IRG penetration threshold was found to be the IRG penetration that the system could successfully handle; all sensitivities were satisfied, and performance was as good as the original case in terms of number of voltage and frequency violations and tie-line limits that were exceeded. Finally, this methodology served as a guide to IRG planners to help them come up with a threshold that is suitable for their system under the constraints that were specified.

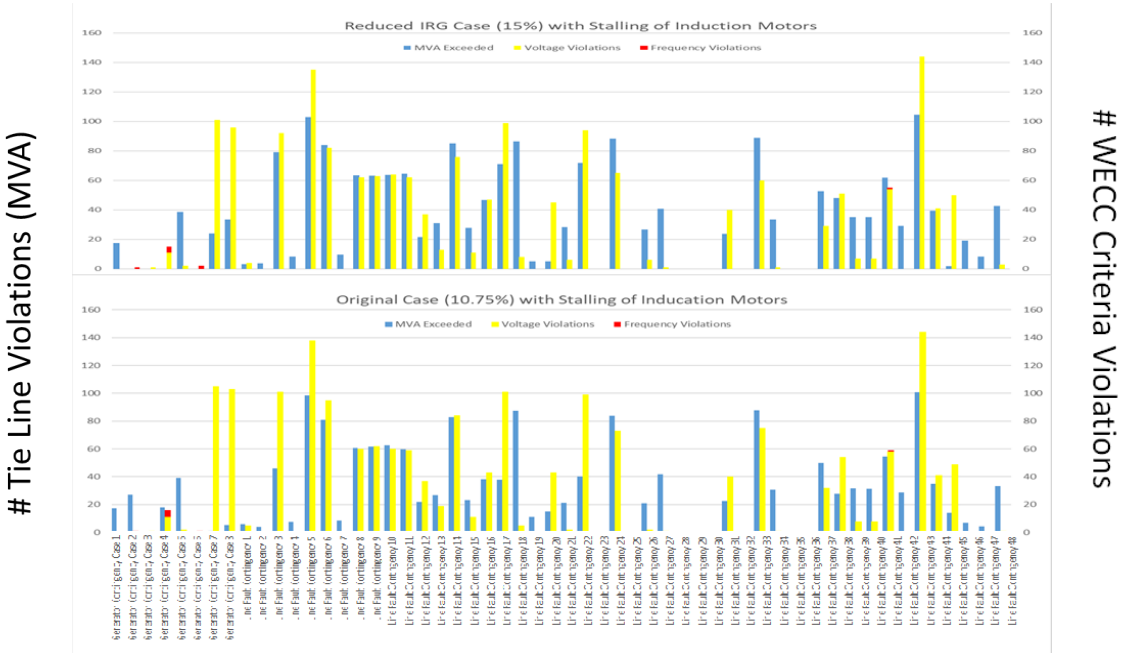

Figure 4.9: Comparison between high IRG case (15%) with stalling of inductions motors modeling and the original case with the same modeling

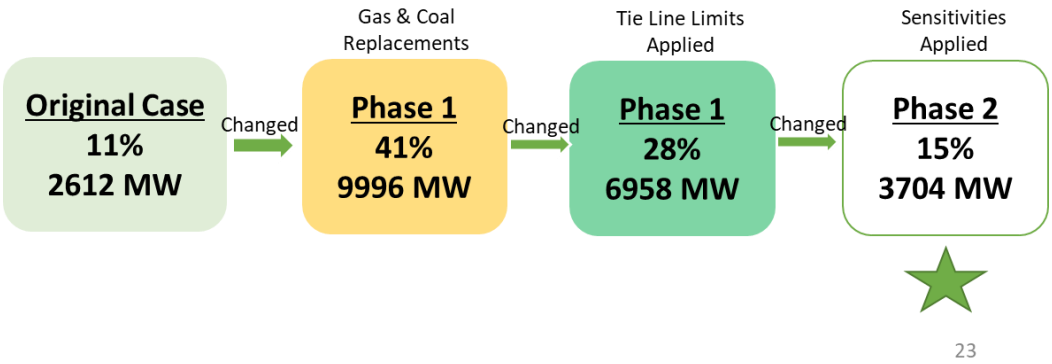

Figure 4.10: The changes of IRG penetration in the case under study throughout Phase 1 and Phase 2

CHAPTER 5
CONCLUSIONS AND FUTURE WORK

The methodology has proven its effectiveness in analyzing the system with minimal use of external simulation programs. Although the system exceeded some of the limits that were specified, it was ensured that the new IRG penetration threshold did not do anything worse than the original case, whose performance was deemed satisfactory. The study done in this thesis also showed that the provided system may not be "perfect" for doing the analysis for which it is given; in such a scenario, the system must be "tweaked" suitably. Awareness of the power system as well as the simulation software are essential to work out a way or a method to overcome the unprecedented issues.

After conducting the methodology on this case study, it was noticed that it is possible to increase the IRG penetration threshold further by doing a more rigorous mathematical analysis. One of the ways to achieve a higher IRG penetration is by the DC Optimal Power Flow (DCOPF). A technique called Lossy DCOPF can be implemented on battery storage locations in the system with renewable energy [52]. Moreover, another related work that can be done is where the proposed IRG units locations in the system be studied historically and use some machine learning technique to decide which locations has more benefits, and whether it will apply less stress on the system [53]. Machine learning has been applied extensively in optimizing the selection and methods used in renewable generation, and with more focus on renewable generation integration, there will always be some improvements in the performance and expansion of green energy. The IRG penetration threshold is expected to reach about 25% after applying the DCOPF and machine learning techniques into the process. Also, the system needs adjustments in the

power flow and dynamic files to avoid the violations and tie line power flow limits excess. More accurate models of the renewable generation units would be a better way to simulate more realistic case and provide output data close to real a world condition.

Overall, the research was conducted to prove that with basic raw data and reasonable knowledge of power system stability, this simple methodology can be followed to achieve reasonably good outcomes. The IRG penetration increased from 11% to 15% mainly due to two reasons in this, which are tie line limits and the sensitivity of stalling of induction motors. The case study was shown to SRP engineers and they agreed on the results that were found. A closer understanding of the effects of stalling of induction motors and more realistic ways of modeling it, were identified as two possible future areas of research by SRP.

REFERENCES

[1] The Electricity Consumers Resource Council (ELCON), "The Economic Impacts of the August 2003 Blackout," 9 February 2004. [Online]. Available: https://www.nrc.gov/docs/ML1113/ML111300584.pdf. [Accessed 9 April 2020].

[2] V. Penmesta and K. Holbert, "Climate Change Effects on Solar, Wind and Hydro Power Generation," in *North American Power Symposium (NAPS)*, Wichita, 2019.

[3] U.S. Energy Information Adminstration , "Electricity explained," 13 December 2019. [Online]. Available: https://www.eia.gov/energyexplained/electricity/electricity-and-the-environment.php. [Accessed 9 April 2020].

[4] Institute for Energy Economics and Financial Analysis, "California tops 2020 goal of 33% renewable energy," 26 February 2019. [Online]. Available: https://ieefa.org/california-tops-2020-goal-of-33-renewable-energy/. [Accessed 9 April 2020].

[5] M. Padhee, A. Pal, M. Mishra and K. Vance, "A fixed-flexible BESS allocation scheme for transmission networks considering uncertainties," *IEEE Transactions on Sustainable Energy*.

[6] C. Mishra, A. Pal, J. Thorp and V. Centeno, "Transient stability assessment of prone-to-trip renewable generation rich power systems using Lyapunov's direct method," *IEEE Trans. Sustainable Energy*, vol. 10, no. 3, pp. 1523-1533, 2019.

[7] C. Mishra, A. Pal and V. Centeno, "Critical clearing time sensitivity for inequality constrained systems," in *Proc. IEEE Power Eng. Soc. General Meeting*, Atlanta, 2019.

[8] D. Nevius, "The History of the North American Electric Reliability Corporation," 2018. [Online]. Available: https://www.nerc.com/AboutNERC/Resource%20Documents/NERCHistory Book.pdf. [Accessed 15 April 2020].

[9] T. Wang, J. Yang, M. Padhee, A. Pal, J. Bi and Z. Wang, "Robust coordinated control of sub-synchronous oscillation in wind integrated power system," *IET Renewable Power Generation*, vol. 14, no. 6, pp. 1031-1043, 2020.

[10] C. Mishra, R. Biswas, A. Pal and V. Centeno, "Critical Clearing Time Sensitivity for Inequality Constrained Systems," *IEEE TRANSACTIONS ON POWER SYSTEMS,* vol. 35, no. 2, pp. 1572-1583, 2020.

[11] C. Wang, M. R, R. Biswas, A. Pal and V. Centeno, "Adaptive LVRT settings adjustment for enhancing voltage security of renewable-rich electric grids," in *IEEE Power Eng. Soc. General Meeting*, Montreal, 2020.

[12] C. Mishra, J. Thorp, V. Centeno and A. Pal, "Transient stability assessment of cascade tripping of renewable sources using SOS," in *Proc. IEEE Power Eng. Soc. General Meeting*, Portland, 2018.

[13] C. Cieslak and L. Grunwald, "Modelling Synthetic Inertia of Wind Turbines for Dynamic Power System Stability Studies," in *54th International Universities Power Engineering Conference (UPEC)*, Bucharest, 2019.

[14] A. Azarpour, S. Suhaimi, G. Zahedi and A. Bahadori, "A Review on the Drawbacks of Renewable Energy as a Promising Energy Source of the Future," *ARABIAN JOURNAL FOR SCIENCE AND ENGINEERING,* vol. 38, no. 2, pp. 317-328, 2012.

[15] M. Padhee, A. Pal, C. Mishra and S. Soni, "Optimal BESS allocation in large transmission networks using linearized BESS models," in *IEEE Power Eng. Soc. General Meeting*, Montreal, 2020.

[16] L. Chow, "Barriers to Renewable Energy Technologies," EcoWatch, 16 February 2018. [Online]. Available: https://www.ecowatch.com/renewable-energy-us-2535432605.html. [Accessed 10 April 2020].

[17] S. S. Refaat, H. Abu-Rub, A. P. Sanfilippo and A. Mohamed, "Impact of grid-tied large-scale photovoltaic system on dynamic voltage stability of electric power grids," *IET Renewable Power Generation,* vol. 12, no. 2, pp. 157-164, 2017.

[18] M. M. Aly, M. Abdel-Akher, Z. Ziadi and T. Senjyu, "Voltage stability assessment of photovoltaic energy systems with voltage control capabilities," in *International Conference on Renewable Energy Research and Applications (ICRERA)*, Nagasaki, 2012.

[19] M. Padhee, A. Pal and K. Vance, "Analyzing effects of seasonal variations in wind generation and load on voltage profiles," in *Proc. IEEE North American Power Symposium (NAPS)*, Morgantown, 2017.

[20] V. Gevorgian, Y. Zhang and E. Ela, "Investigating the Impacts of Wind Generation Participation in Interconnection Frequency Response," *IEEE Transactions on Sustainable Energy,* vol. 6, no. 3, pp. 1004 - 1012, 2015.

[21] T. Wang, J. Yang, J. Liu, P. Gupta, A. Pal and J. Deng, "SDAE-based probabilistic stability analysis of wind integrated power systems".

[22] C. Mishra, J. Thorp, V. Centeno and A. Pal, "Estimating relevant portion of stability region using Lyapunov approach and sum of squares," in *Proc. IEEE Power Eng. Soc. General Meeting,* Portland, 2018.

[23] C. Mishra, J. Thorp, V. Centeno and A. Pal, "Stability region estimation under low voltage ride through constraints using sum of squares," in *Proc. IEEE North American Power Symposium (NAPS),* Morgantown, 2017.

[24] California Energy Commission, "RPS Eligibility Guidebook, Ninth Edition Revised," 27 April 2017. [Online]. Available: https://efiling.energy.ca.gov/getdocument.aspx?tn=217317. [Accessed 10 April 2020].

[25] N. Lee, F. Flores-Espino and D. Hurlbut, "RENEWABLE ENERGY ZONE (REZ): A GUIDEBOOK FOR PRACTITIONERS," September 2017. [Online]. Available: https://www.nrel.gov/docs/fy17osti/69043.pdf. [Accessed 10 April 2020].

[26] M. Barkakati and A. Pal, "A comprehensive data driven outage analysis for assessing reliability of the bulk power system," in *Proc. IEEE Power Eng. Soc. General Meeting,* Atlanta, 2019.

[27] R. Karki, P. Hu and R. Billinton, "A Simplified Wind Power Generation Model for Reliability Evaluation," *IEEE Transactions on Energy Conversion,* vol. 21, no. 2, pp. 533 - 540, 2006.

[28] A. Moreira, D. Pozo and A. S. E. Street, "Reliable Renewable Generation and Transmission Expansion Planning: Co-Optimizing System's Resources for Meeting Renewable Targets," *IEEE TRANSACTIONS ON POWER SYSTEMS,* vol. 32, no. 4, pp. 3246-3257, 2017.

[29] F. D. Muniz, B. F. Hobbs, J. L. Ho and S. Kasina, "An Engineering-Economic Approach to Transmission Planning Under Market and Regulatory Uncertainties: WECC Case Study," *IEEE TRANSACTIONS ON POWER SYSTEMS,* vol. 29, no. 1, pp. 307-317, 2014.

[30] L. L. Garver, "Transmission Network Estimation Using Linear Programming," *IEEE TRANSACTIONS ON POWER APPARATUS AND SYSTEMS,* Vols. PAS-89, no. 7, pp. 1688-1697, 1970.

[31] P. G. Bueno, J. C. Hernández and F. J. Ruiz-Rodriguez, "Stability assessment for transmission systems with large utility-scale photovoltaic units," *IET Renewable Power Generation,* vol. 10, no. 5, pp. 584 - 597, 2015.

[32] I. Pena, C. Brancucci Martinez-Anido and B.-M. Hodge, "An Extended IEEE 118-Bus Test System With High Renewable Penetration," *IEEE TRANSACTIONS ON POWER SYSTEMS,* vol. 33, no. 1, pp. 281 - 289, 2018.

[33] A. Marini Mohamad and N. Abdul Rashid, "Power System Stability analysis using Integration of Prony, PSSE, Python and Excel," in *International Computer Science and Engineering Conference (ICSEC)*, Bangkok, 2017.

[34] M. Nouha and B. Chokri, "Analysis and Evaluation of Phtovoltaic Integration Impacts in Tunisian Grid USING PSSE," in *International Renewable Energy Congress*, Hammamet, 2018.

[35] J. Tong and L. Wang, "Design of a DSA Tool for Real Time System Operations," in *International Conference on Power System Technology*, Chongqing, 2006.

[36] L. Ding, A. Xue, F. Han, J. Li, M. Wang, T. Bi and J. Wang, "Dominant Mode Identification for Low Frequency Oscillations of Power Systems based on Prony Algorithm," in *International Conference on Critical Infrastructure*, Beijing, 2010.

[37] S. Li, "Unnoticed Differences in PSS/E and PSLF Format — 2nd Generation Generic Renewable Energy Model," January 2019. [Online]. Available: https://www.wecc.org/Administrative/Unnoticed%20Differences%20in%20PSSE%20and%20PSLF%20Models-%20Li.pdf. [Accessed 10 April 2020].

[38] S. Varadan, G. Freddo, H. Todus, J. Thiemsuwan, K. Chen, D. Hawkins and S. Shen, "A New Approach to Studying the Impact of Intermittent Renewable Resources," in *IEEE Power and Energy Society General Meeting*, San Diego, 2012.

[39] V. Ajjarapu and K. K. Yagnik, "Consideration of the wind and solar generation reactive power capability on grid voltage performance," in *IEEE Power and Energy Society General Meeting*, San Diego, 2012.

[40] R. Elliott, R. Byrne, A. Ellis and L. Grant, "Impact of Increased Photovoltaic Generation on Inter-area Oscillations in the Western North American Power

System," in *IEEE PES General Meeting | Conference & Exposition*, National Harbor, 2014.

[41] K. Clark, A. Walling and N. W. Miller, "Solar photovoltaic (PV) plant models in PSLF," in *IEEE Power and Energy Society General Meeting*, Detroit, 2011.

[42] NERC, "Reliability Guideline Power Plant Dynamic Model Verification using PMUs," September 2016. [Online]. Available: https://www.nerc.com/comm/PC_Reliability_Guidelines_DL/Reliability%20Guideline%20%20Power%20Plant%20Model%20Verification%20using%20PMUs%20-%20Resp.pdf. [Accessed 10 April 2020].

[43] R. Walton, "NERC: Grid operators must prepare for 330 GW of renewables by 2029," Utility Dive, 30 Decmeber 2019. [Online]. Available: https://www.utilitydive.com/news/nerc-grid-operators-must-prepare-for-330-gw-of-renewables-by-2029/569462/. [Accessed 19 April 2020].

[44] J. Hein, D. Hurlbut, M. Milligan, L. Coles and B. Green, "Transmission Planning Process and Opportunities for Utility-Scale Solar Engagement within the Western Electricity Coordinating Council (WECC)," National Renewable Energy Laboratory, November 2011. [Online]. Available: https://www.nrel.gov/docs/fy12osti/51279.pdf. [Accessed 10 April 2020].

[45] WECC, "System Performance TPL-001-WECC-CRT-2.1 Regional Criterion," 25 June 2014. [Online]. Available: https://www.wecc.org/Reliability/TPL-001-WECC-CRT-2.1.pdf. [Accessed 10 April 2020].

[46] WECC, "WECC Criterion TPL-001-WECC-CRT-3.1," 6 December 2016. [Online]. Available: https://www.wecc.org/Reliability/TPL-001-WECC-CRT-3.1.pdf. [Accessed 12 April 2020].

[47] K. Raviteja, P. Kumar Kar and S. Bhaskar Karanki, "Renewable Energy Resources Integration To Grid With Improved Power Quality Capabilities And Optimal Power Flows," in *IEEE International Conference on Power Electronics, Drives and Energy Systems (PEDES)*, Chennai, 2019.

[48] M. V. Venkatasubramanian, Y. Li and Y. Chen, "Coordination of Transmission Line Final Project Report," May 2002. [Online]. Available: https://pserc.wisc.edu/documents/publications/reports/2002_reports/S-8_Final-Report_April-2003.pdf. [Accessed 10 April 2020].

[49] NERC, "1,200 MW Fault Induced Solar Photovoltaic Resource Interruption Disturbance Report," June 2017. [Online]. Available: https://www.nerc.com/pa/rrm/ea/1200_MW_Fault_Induced_Solar_Photovoltaic_Resource_/1200_MW_Fault_Induced_Solar_Photovoltaic_Resource_Interruption_Final.pdf. [Accessed 11 April 2020].

[50] M. Padhee and A. Pal, "Effect of solar PV penetration on residential energy consumption pattern," in *2018 North American Power Symposium (NAPS)*, Fargo, 2018.

[51] NERC, "Technical Reference Document Dynamic Load Modeling," December 2016. [Online]. Available: https://www.nerc.com/comm/PC/LoadModelingTaskForceDL/Dynamic%20Load%20Modeling%20Tech%20Ref%202016-11-14%20-%20FINAL.PDF. [Accessed 11 April 2020].

[52] A. Castillo, Jiang, Xinyi and D. F. Gayme, "Lossy DCOPF for Optimizing Congested Grids with Renewable Energy," in *American Control Conference (ACC)*, Portland, 2014.

[53] W. Fumiya, T. Kawaguchi, T. Ishizaki, H. Takenaka, T. Y. Nakajima and J.-i. Imura, "Machine Learning Approach to Day-ahead Scheduling for Multiperiod Energy Markets under Renewable Energy Generation Uncertainty," in *IEEE Conference on Decision and Control (CDC)*, Miami, 2018.

APPENDIX A

PROGRAM 1: EPCL CODE TO EXTRACT THE REACTIVE POWER OUT OF A CHANNEL FILE

```
##############################################################################
#
# Program Name: Reactive Power extractor from model "imetr"
#
# Description: Extracts the reactive power collected by the model "imetr"
#
#
# Author: Hashem Albhrani
# Arizona State University
#
# Last Modified: 2/15/2020 %
#
##############################################################################


dim *filename[30][1000]
dim *outfile[2][1000]
dim #ord[4012]
dim #abc[4012]
dim #time[4012]
dim #data[4012][180]
dim #busnum[4012]
@count=0
@flag=0
*filename[0]="D:\Hashem Dynamic Contingency Files Feb 19
current\output\Contingency_Case1.chf"


for @k=0 to 0
*outfile[0]=*filename[@k]+"qbr.csv"
@return = openlog(*outfile[0])
@ret=getp(*filename[@k])
If( @ret < 0 )
logterm("Cannot open the chf file”)
end
else
@num = @ret  /* find the number of points */
endif
logterm("# of records = ",@num,"<")
for @i = 0 to plotpar[0].nchan-1
if ((channel[@i].typec = "qbr") and (channel[@i].modelname = "imetr"))

@count=@count+1
$n = format(channel[@i].bus,8,0)
```

```
#busnum[@count]=channel[@i].bus

@ch = getchan(channel[@i].pselect,channel[@i].cid,channel[@i].typec,@num)
for @j= 0 to @num-1
#time[@j]=#abc[@j]:10:4
#data[@j][@count-1]=#ord[@j]:10:4
next
endif
next


for @i=0 to @count
logprint(*outfile[0],",",#busnum[@i])
next
logprint(*outfile[0],"<")
for @i= 0 to @num-1
logprint(*outfile[0],",",#time[@i])
for @kk=0 to @count-1
logprint(*outfile[0],",",#data[@i][@kk])/**/
next
logprint(*outfile[0],"<")
next
@count=0

next
```

APPENDIX B

PROGRAM 2: EPCL CODE TO EXTRACT THE REAL POWER OUT OF A CHANNEL FILE

```
#########################################################################
#
# PROGRAM NAME: REAL POWER EXTRACTOR FROM MODEL "IMETR"
#
# DESCRIPTION: EXTRACTS THE REAL POWER COLLECTED BY THE MODEL
"IMETR"
#
#
# AUTHOR: HASHEM ALBHRANI
# ARIZONA STATE UNIVERSITY
#
# LAST MODIFIED: 2/15/2020 %
#
#########################################################################


DIM *FILENAME[30][1000]
DIM *OUTFILE[2][1000]
DIM #ORD[4012]
DIM #ABC[4012]
DIM #TIME[4012]
DIM #DATA[4012][180]
DIM #BUSNUM[4012]
@COUNT=0
@FLAG=0
*FILENAME[0]="D:\HASHEM DYNAMIC CONTINGENCY FILES FEB 19
CURRENT\OUTPUT\P7_SRPWGDEERWG.CHF"


FOR @K=0 TO 0
*OUTFILE[0]=*FILENAME[@K]+"PBR.CSV"
@RETURN = OPENLOG(*OUTFILE[0])
@RET=GETP(*FILENAME[@K])
IF( @RET < 0 )
LOGTERM("CANNOT OPEN THE CHF FILE”)
END
ELSE
@NUM = @RET  /* FIND THE NUMBER OF POINTS */
ENDIF
LOGTERM("# OF RECORDS = ",@NUM,"<")
FOR @I = 0 TO PLOTPAR[0].NCHAN-1
IF ((CHANNEL[@I].TYPEC = "PBR") AND (CHANNEL[@I].MODELNAME =
"IMETR"))

@COUNT=@COUNT+1
```

```
$N = FORMAT(CHANNEL[@I].BUS,8,0)

#BUSNUM[@COUNT]=CHANNEL[@I].BUS

@CH =
GETCHAN(CHANNEL[@I].PSELECT,CHANNEL[@I].CID,CHANNEL[@I].TYPEC,
@NUM)
FOR @J= 0 TO @NUM-1
#TIME[@J]=#ABC[@J]:10:4
#DATA[@J][@COUNT-1]=#ORD[@J]:10:4
NEXT
ENDIF
NEXT


FOR @I=0 TO @COUNT
LOGPRINT(*OUTFILE[0],",",#BUSNUM[@I])
NEXT
LOGPRINT(*OUTFILE[0],"<")
FOR @I= 0 TO @NUM-1
LOGPRINT(*OUTFILE[0],",",#TIME[@I])
FOR @KK=0 TO @COUNT-1
LOGPRINT(*OUTFILE[0],",",#DATA[@I][@KK])/**/
NEXT
LOGPRINT(*OUTFILE[0],"<")
NEXT
@COUNT=0

NEXT
```

APPENDIX C

PROGRAM 3: TIE LINE POWER FLOW ANALYZER

```
#############################################################################
#
# Program Name: Tie Line Power Flow Analyzer
#
# Description: Analyze the extracted power flow data for both reactive
# and real power from the channel files generated after simulating
# the contingency case with “imetr” model added
#
# Author: Hashem Albhrani
# Arizona State University
#
# Last Modified: 3/13/2020 %
#
#############################################################################

import pandas as pd
import numpy as np

df = pd.read_csv('D:\Hashem Dynamic Contingency Files Feb 19 current\limits.csv')
qbr = pd.read_csv('D:\Hashem Dynamic Contingency Files Feb 19
current\output\Contingency_Case1.chfqbr.csv')
qbr =
qbr[['14002','14003','14012','14021','14101','14101.1','14101.2','14101.3','14108','14201','
14209','14209.1','14211','14221','14222','14223','14226','14231','14231.1','14243','14246','
14250','14258','14260','14265','14301','14303','14350','14356','14356.1','14357','14359','14
360','14534','14597','14598','14599','14606','14616','14617','14619','15021','15034','15090'
,'15090.1','15090.2','15211','15211.1','15212','15212.1','15230','15232','15271','15272','15
284','15288','15292','15613','16101','16102','16102.1','16102.2','16102.3','16104','16350','1
6351','16352','16353','16354','16355','16356','16357','16415','16804','16804.1','16837','168
38','16935','17001','17012','17023','17087','17103','17103.1','17172','17174','17175','17176
','17177','17178','17179','17180','17181','17182','17185','17186','17187','17188','17189','17
430','17608','17620','19017','19600','84810','84819','84836','84836.1','84846','84846.1','84
846.2','84859','84895','85780','85811','85993','85993.1','92520','159030']]

pbr = pd.read_csv('D:\Hashem Dynamic Contingency Files Feb 19
current\output\Contingency_Case1.chfpbr.csv')
pbr =
pbr[['14002','14003','14012','14021','14101','14101.1','14101.2','14101.3','14108','14201','
14209','14209.1','14211','14221','14222','14223','14226','14231','14231.1','14243','14246','
14250','14258','14260','14265','14301','14303','14350','14356','14356.1','14357','14359','14
360','14534','14597','14598','14599','14606','14616','14617','14619','15021','15034','15090'
,'15090.1','15090.2','15211','15211.1','15212','15212.1','15230','15232','15271','15272','15
284','15288','15292','15613','16101','16102','16102.1','16102.2','16102.3','16104','16350','1
6351','16352','16353','16354','16355','16356','16357','16415','16804','16804.1','16837','168
38','16935','17001','17012','17023','17087','17103','17103.1','17172','17174','17175','17176
```

```
','17177','17178','17179','17180','17181','17182','17185','17186','17187','17188','17189','17
430','17608','17620','19017','19600','84810','84819','84836','84836.1','84846','84846.1','84
846.2','84859','84895','85780','85811','85993','85993.1','92520','159030']]

#mva = pd.DataFrame(columns = ['MVA'])

comp=[]
comp1 = []
comp2 = []
comp_exced = []
comp_exced_limit = []
loccc_new = 0
mva_df = 0
mva_df_current = []
mva_exceds_values = []
final_exceeding_value_table = []
mva_max_voilation = []
mva_df_current_last = []

comp2 = pd.DataFrame(comp2)
final_exceeding_value_table = pd.DataFrame(final_exceeding_value_table)
mva_max_voilation = pd.DataFrame(mva_max_voilation)
comp_exced = "weren't Exceeded"

for loccc in np.arange(0,118):
    mva = pd.DataFrame(columns = ['MVA'])
    #print (loccc)
    mva['MVA'] = pd.DataFrame(np.sqrt(qbr.iloc[:,loccc]**2+pbr.iloc[:,loccc]**2))
    mva = mva.iloc[460:]
    #print (mva)

    mva_excds_values = []
    mva_df_current_last = []
    comp1 = []
    mva_df = 0
    mva_df_current = 0


    for i in mva['MVA']: #Value of MVA to be compared
        mva_df = 0
        if(df['MVA2'][loccc]>i):
            comp1.append(0)

        else:
            mva_df = i - df['MVA2'][loccc]
```

```
            mva_excds_values.append(mva_df)

            comp1.append(mva_df)
            comp_exced = "Were Exceeded! (Violation)"

            if (loccc > loccc_new):
                  loccc_new = loccc
                  comp_exced_limit.append(loccc_new)
                  final_exceeding_value_table [loccc] = mva_excds_values
            if (mva_df > mva_df_current):
                  mva_df_current = mva_df
                  mva_df_current_last.append(mva_df)
      #mva_max_voilation [loccc] = mva_df_current_last
      comp2 [loccc] = comp1

comp2['Total'] = comp2.sum(axis=1)
max_time_voild = (str(comp2['Total'].idxmax()))
max_time_voild_value = str(comp2["Total"].max())
max_time_voild_value = "{0:.2f}".format(float(max_time_voild_value))

comp = pd.DataFrame(comp2)
print("")
print("Limits " + comp_exced + " the most at time (row) " + "# " + max_time_voild + "
#" )
print("")
print("Amount of Max Voilation " + "@ " + max_time_voild_value + " @")
print("")
print ("Buses violated Limits Below: ")
print (comp_exced_limit)
#comp.to_csv('C:/Users/halbhran/Desktop/comparison1.csv')
```